The Massachusetts Bay Hydrodynamic Model: 2005 Simulation

Massachusetts Water Resources Authority
Environmental Quality Department
Report ENQUAD 2008-12

Jiang MS, Zhou M. 2008. **The Massachusetts Bay Hydrodynamic Model: 2005 Simulation**. Boston: Massachusetts Water Resources Authority. Report 2008-12. 58 pp.

Massachusetts Water Resources Authority
Boston, Massachusetts

The Massachusetts Bay Hydrodynamic Model: 2005 Simulation

Prepared by:
Mingshun Jiang & Meng Zhou
Department of Environmental, Earth and Ocean Sciences
University of Massachusetts Boston
100 Morrissey Blvd
Boston, MA 02125

July 2008

EXECUTIVE SUMMARY

The Boston Harbor, Massachusetts Bay and Cape Cod Bay system (MBS) is a semi-enclosed coastal system connected to the Gulf of Maine (GOM) through boundary exchange. Both natural processes including climate change, seasonal variations and episodic events, and human activities including nutrient inputs and fisheries affect the physical and biogeochemical environment in the MBS. Monitoring and understanding of physical–biogeochemical processes in the MBS is important to resource management and environmental mitigation.

Since 1992, the Massachusetts Water Resource Authority (MWRA) has been monitoring the MBS in one of the nation's most comprehensive monitoring programs. Under a cooperative agreement between the MWRA and University of Massachusetts Boston (UMB), the UMB modeling team has conducted numerical simulations of the physical–biogeochemical conditions and processes in the MBS during 2000-2004. Under a new agreement between MWRA, Battelle and UMB, the UMB continues to conduct a numerical simulation for 2005, a year in which the MBS experienced an unprecedented red–tide event that cost tens of millions dollars to Massachusetts shellfish industry. This report presents the model validation and simulated physical environment in 2005.

The results from the hydrodynamic model run for 2005, for example, temperature, salinity and currents, are well compared with observations from moorings and field surveys, and are of similar quality as model results of 2000–2004. Modeled results show short–term variability and seasonal changes in temperature, salinity, and circulation responding to short–term and seasonal meteorological forcing, freshwater runoff and the GOM forcing. Specifically, this report will address two important processes: (1) cooling and mixing process in winter and (2) freshwater plumes from the GOM into MB coast in spring through comparisons between model results, satellite SST images, and field survey data.

This study also focused on the physical environment and circulation in the MBS during the unusual Nor'easter storms in May 2005 to gain an understanding of how the MBS responds to strong northeasterly winds and strong GOM coastal currents. Model results and available physical and biogeochemical data suggest that Ekman transport and wind–induced vertical mixing are important factors determining water exchanges between the MBS and GOM and nutrient supplies to the upper water column. The model also reproduced well coastal plumes, currents, and eddies south of Cape Ann, which are important processes for transport and retention of nutrients and biota.

The model continues to experience difficulties in the comparison between observations and simulations of (1) summer processes including bottom currents and response to upwelling/downwelling and (2) the magnitude, spatial pattern, and timing of responses to short-term events.

The discrepancies between model results and observations in temperature, salinity and currents in the MBS indicate the limitations in both the model and monitoring results. The discrepancies can provide guidance for revising the monitoring program and developing data assimilation methods to improve model performance. For example, the paucity of observations at the open boundary results in an over-smoothed open boundary

condition. This caused inaccuracies in modeled water exchanges between the MBS and GOM, and in modeled salinity during spring. However, additional data were available in spring 2005 from field surveys added by MWRA and Woods Hole Oceanographic Institution (WHOI) in response to the red-tide bloom. This allowed us to construct better boundary conditions and improve the model results.

TABLE OF CONTENTS

LIST OF FIGURES

LIST OF TABLES

1. INTRODUCTION

1.1 Project overview

The Boston Harbor (BH), Massachusetts Bay (MB) and Cape Cod Bay (CCB) system (MBS) is important to the regional economy by serving a busy commercial harbor, a productive fishing ground, a critical habitat of endangered North Atlantic Right whales and a prosperous tourism industry. A healthy marine environment is important to the more than three million people living in the surrounding area. Significant efforts have been made to clean up Boston Harbor in the last decades. The construction of the Deer Island wastewater treatment plant and the relocation of the effluent outfall from Deer Island to 15 km offshore were among the biggest human efforts in the nation to restore an urbanized harbor.

Under the long-term Cooperative Research Agreement signed in 2001 between the University of Massachusetts Boston (UMB) and Massachusetts Water Resources Authority (MWRA), the UMB provided both hydrodynamics and water quality model run results for 2000–2004 to the MWRA (Zhou, 2002; Jiang and Zhou, 2003; Jiang and Zhou, 2004a,b, 2006a,b). The hydrodynamic model for the MBS was constructed by the U.S. Geological Survey (USGS) in Woods Hole based on the ECOM-si developed by HydroQual Inc. (HydroQual) (Signell et al., 1996). The Water Quality Model was developed by HydroQual (HydroQual, 2000). This current project for the 2005 hydrodynamic and water quality model runs is under the subcontract of Battelle, which is leading the monitoring program in the MBS. While conducting the model run, we focused on:

1) Studying the physical mechanisms determining the intruding GOM coastal current into MB.
2) Studying the formation and translation of mesoscale eddies near the north shore and their impacts on transport and retention of nutrients and biota.

1.2 Physical setting

The MBS is a semi-enclosed embayment located in the western Gulf of Maine (GOM) and surrounded by the Boston metropolitan region to the north and west, and Cape Cod to the south (Figure 1.1). The MBS is about 100 km long and 50 km wide, and has an average depth of 35 m.

Stellwagen Basin is the only deep basin in the MBS with a maximum depth up to 90 m. It is bounded in the east by Stellwagen Bank with the shallowest depth of about 20 m. Thus the MBS is connected to the GOM mostly through the North Passage off Cape Ann and the South Passage off Race Point.

Previous studies have indicated that the circulation in the MBS varies in response to short– and long–term local and remote forcing including 1) wind stresses and heat fluxes at the sea surface, 2) tides and mean surface slopes at the open boundary, and 3) freshwater runoff including outfall effluent (Geyer et al., 1992; Signell et al., 1996; Jiang and Zhou, 2004a; Jiang and Zhou, 2006a). The yearly mean current in the MBS is characterized by a counterclockwise circulation, which is primarily driven by the GOM intruding current through the North Passage, local freshwater runoff, and surface heating. Tides are dominated by the semidiurnal M_2 constituent. Tidal currents vary from 10 cm s^{-1} in the Stellwagen Basin, to 50 cm s^{-1} in the South Passage. The water column stratification varies seasonally. Stratification occurs in spring due to both freshwater runoff and surface heating, which is intensified and reaches a maximum strength during summer. The water column is de-stratified during fall due to surface cooling and increasing wind mixing, and is well mixed in winter.

As early as 1927, Bigelow suggested that the western Maine Coastal Current (WMCC) breaks into two branches at Cape Ann: one intrudes deeply into the MBS, and another follows the outer edge of the Stellwagen Bank (Bigelow, 1927; Lynch et al., 1996). This bifurcation is determined by the nonlinear interaction between topography, coastal lines, baroclinic fields strongly influenced by freshwater runoff from the Merrimack River and the WMCC. The volume transport of this intruding current primarily determines the circulation in the MBS. It circulates counterclockwise along western Massachusetts Bay and frequently penetrates into CCB, especially in winter and spring seasons (Geyer et al., 1992; Jiang and Zhou, 2004a).

Previous studies indicated pronounced seasonal variations in the circulation pattern (Geyer et al., 1992; HydroQual and Signell, 2001; Signell et al., 1996; Butman, et al., 2002; Jiang and Zhou, 2004a). In western MB, surface currents are strongly driven by winds. In winter and spring seasons, northerly winds drive a southward coastal current creating a counterclockwise circulation. During the summer and early fall, predominantly southwesterly winds produce offshore Ekman transport and coastal upwelling, which induce a northward coastal current along the upwelling front at the western coast.

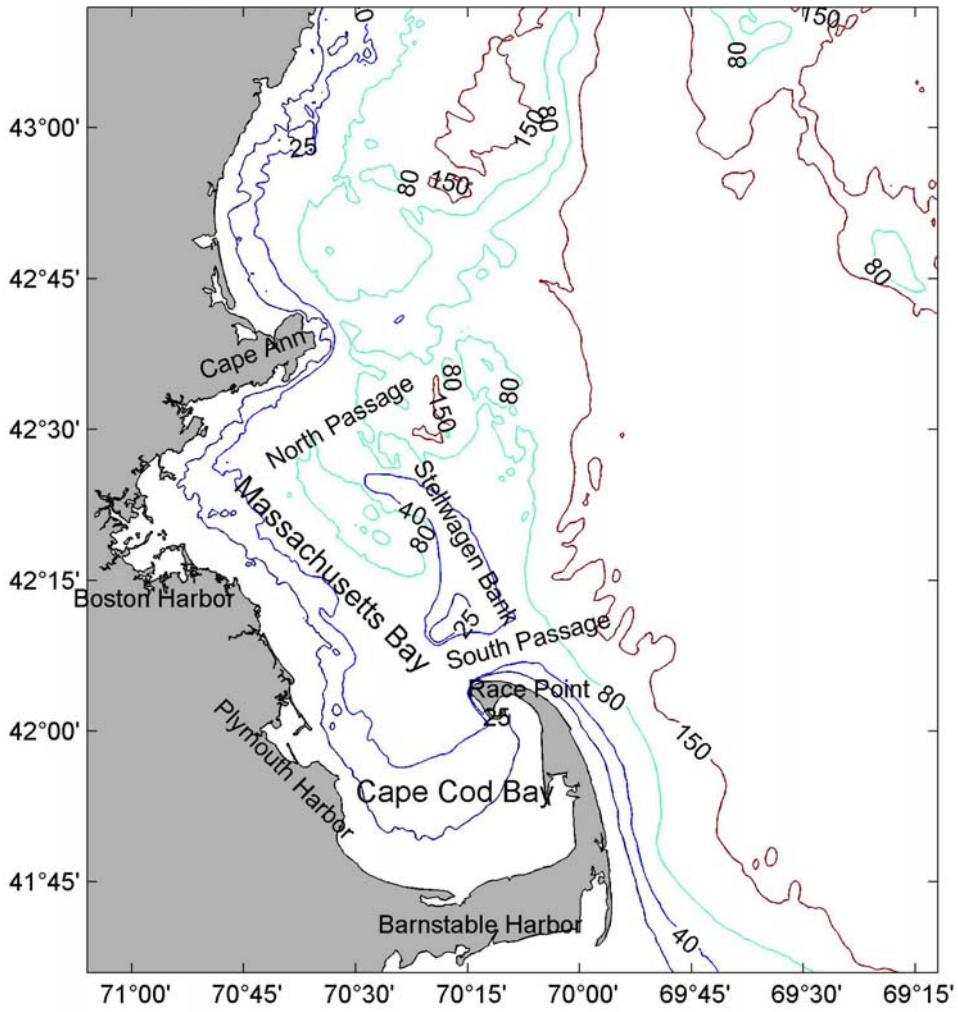

Figure 1.1. Bathymetry in Boston Harbor, Massachusetts Bay and Cape Cod Bay.

2. MODEL DESCRIPTION

A brief model description is presented in this section. Table 2.1 and Table 2.2 list the model prognostic variables and values of key parameters, and Table 2.3 lists the frequencies and filters of forcing data, validation data, and model output. More details of this model, such as the basic model equations and treatment of solar radiation, can be found in earlier reports (Signell et al., 1996, HydroQual and Signell, 2001). In the 2005 simulation, we used the same model implementation (parameters, forcing data frequencies, boundary conditions, etc.) as in 2002-2004 simulations including the data assimilation of measurements at the GoMOOS buoy B (Figure 2.1).

2.1 Numerical schemes

The Massachusetts Bay and Cape Cod Bay hydrodynamic model is based on the semi-implicit Estuarine, Coastal and Ocean Model (ECOM-si), which is a derivative of the Princeton Ocean Model (POM) (Blumberg and Mellor, 1987; Signell et al., 1996). The model solves the three-dimensional primitive equations using a terrain-following coordinate (sigma coordinate) and a semi-implicit scheme developed by Casulli et al. (1990) in the calculation of the free sea surface elevation to avoid the splitting of barotropic and baroclinic modes. The integration of passive tracer equations is further enhanced by using an anti-diffusion algorithm (Smolarkiewicz et al., 1984).

The vertical turbulent closure is the Mellor-Yamada Level 2 ½ scheme (Mellor and Yamada, 1982) with modifications by Galperin et al. (1988), while the horizontal mixing is parameterized as formulated by Smagorinsky (1963). In addition to turbulent mixing, a background vertical mixing is chosen as 5×10^{-6} m^2 s^{-1}. Moreover, a Shapiro filter is applied to the velocity field every 2 hours to remove the 2 grid-length variability (Shapiro, 1975).

2.2 Model domain and grids

The model domain extends into the GOM with an open boundary from Portsmouth, NH to offshore of Cape Cod, MA. The domain includes the Merrimack River, the largest source of fresh water in the region (Figure 2.1). This configuration minimizes the influences of inaccurate boundary conditions due to insufficient data in the construction of open boundary conditions. The bottom topography is smoothed with the maximum depth of 140 m near the eastern

boundary and the minimum depth of 3 m near coastal areas to avoid treating flooding and drying grids.

The model has 68×68 grids with the grid spacing approximately from 600 m in Boston Harbor to about 6 km along the open boundary. Vertically, the model has 12 sigma levels with the upper three levels located at 0.01, 0.04 and 0.1 sigma depths, and the remaining 9 layers at a 0.1 sigma depth interval evenly distributed over the rest of water column.

2.3 Time step

A time step of 207 seconds is used throughout the entire simulation between years 2002 and 2004. Though the semi-implicit scheme used for the sea surface elevation avoids the instability of an explicit scheme produced by the gravity waves, the model time step is limited by the advective Courant-Levis-Frederick (CFL) condition, which requires the modeled time step less than or equal to grid spacing divided by current speed ($\Delta t \leq \Delta x/U$). A time step of 207 seconds is a very conservative choice. The model was executed stably.

2.4 Forcing

2.4.1 Surface forcing

The surface forcing includes wind stresses, incoming short wave radiation, net outgoing long wave radiation, sensible heat fluxes and latent heat fluxes. The freshwater input at the surface was set to zero because there were no measurements of precipitation and evaporation at offshore stations. Precipitation was measured at Logan Airport, but evaporation was not. Thus a wet or dry year was reflected in river discharges. Wind stresses and heat fluxes were calculated based on meteorological measurements made at NOAA buoy 44013 and solar radiation measurements at Woods Hole Oceanographic Institution (Figure 2.2). As with previous year's runs, we did not correct the anemometer height from 5m to the standard 10m height required by the model. For relative humidity, we continued previous years' practice of using measurements from Logan Airport in the calculation of sensible and latent heat fluxes. The wind stresses were calculated using the Large and Pond formulation (Large and Pond, 1981), and long wave radiation, sensible and latent heat fluxes were calculated using the formulation developed by Weller et al. (1995).

The meteorological forcing is typical of mid-latitude regions: in fall and winter, northerly wind is dominant with a wind speed frequently exceeding 10 m s^{-1}; and in spring and summer, southerly wind is dominant with an overall wind speed less than 5 m s^{-1}. The air temperature is

lowest (well below -10ºC) in January and highest in July and August reaching 25ºC. In 2005, winter temperature was mild most of the time except in late January, when temperature was below -10ºC for two weeks. This year was unusual because there were two Nor'easters in May (Figure 2.2b). These types of weather events normally hit the region in fall and winter.

Solar radiation penetrates into the water column. The absorption of short wave radiation is computed as a function of water depth, i.e.

$$I(z) = I_0 \exp(-k_e z) \tag{2.1}$$

where I_0 is the solar radiation at the sea surface, k_e is the light attenuation coefficient, z is the water depth, and $I(z)$ is the solar radiation at depth z. The value of k_e is calculated based on light transmissivity data collected during the outfall monitoring program and is spatially variable ranging from 0.6 m^{-1} in Boston Harbor to 0.16 m^{-1} offshore (HydroQual and Signell, 2001). The same values of k_e were used in 2005 simulation because no significant change in the Boston Harbor water clarity was observed during the three-year surveys (2001-2003) after the outfall relocation (Taylor, 2005).

2.4.2 Freshwater inputs

There are four major land sources of freshwater, the Merrimack River, Charles River, Neponset River, and MWRA sewage effluent (Figures 2.3). Among them, the Merrimack River is the largest with an averaged flux of 200 $m^3 s^{-1}$, while the other sources are much smaller with an averaged flux of ~20 $m^3 s^{-1}$. All river discharges have strong seasonality with the maximum runoff between late March and early May. In 2005, all rivers saw record-high discharges during their peak periods, which occurred in April, earlier than normal years. The rivers also had record-high discharges in October-November (http://www.fema.gov/news/event.fema?id=5206).

The effluent from the MWRA Deer Island facility has been completely diverted to the new outfall site in Massachusetts Bay since September 2000. The effluent flow from the MWRA Deer Island facility has been nearly constant throughout these years with episodic events of relatively high flows. As with model runs for previous years, the runoff from the Mystic River was included in the model freshwater source even though it is small; the sewage flux from South Essex plant flow was not included because it is less than 1.3 $m^3 s^{-1}$. Daily mean flows of these rivers were used for model inputs.

2.4.3 Open boundary conditions

Open boundary conditions required by the model include surface elevation, temperature and salinity. Surface elevation consists of tidal and low frequency components. The low frequency surface slope determines the geostrophic currents normal to the boundary. Different from earlier simulations, the tidal elevation for 2005 is derived from a regional tidal model (ADCIRC) (Hagen and Parrish, 2004).

An objective interpolation procedure is used to derive the temperature and salinity along the open boundary, which is similar to the interpolation procedure in the previous simulations (HydroQual and Signell, 2001). The interpolation software, called OAX, is developed by Bedford Institute of Oceanography (http://www.mar.dfo-mpo.gc.ca/science/ocean/coastal_hydrodynamics/oax.html). The interpolation is made by weighting available data onto the open boundary based on a specified statistical correlation function of horizontal distance, depth and time, so that the statistical interpolation error is known. The correlation function is as follows,

$$R(r) = \left(1 + r + \frac{r^3}{3}\right)\exp(-r) \tag{2.2}$$

where r is the pseudo-distance between the data point and the target point,

$$r = \sqrt{\left(\frac{x - x_0}{a}\right)^2 + \left(\frac{y - y_0}{a}\right)^2 + \left(\frac{z - z_0}{b}\right)^2 + \left(\frac{t - t_0}{T}\right)^2} \tag{2.3}$$

where a, b, and T are the horizontal (30 km), vertical (15 m) and temporal (20 day) correlation scales respectively. The pseudo-distance controls the selection of nearest points for interpolation. The RMS represents the relative estimation error, defined as the square-root of the error variance by interpolation, and is scaled from 0 to 1.

Temperature and salinity measurements from the National Marine Fisheries Service (NMFS), MWRA, Woods Hole Oceanographic Institution (WHOI), University of New Hampshire (UNH), and Stellwagen Bank National Marine Sanctuary (SBNMS) were compiled based on latitude, longitude, depth, and time. For example, the monthly station maps in April and in August for available data are shown in Figures 2.4. The monthly data coverage varies significantly in space and time, and is summarized in Table 2.1.

The same procedure for calculating the low frequency surface elevation along the open boundary in the 2000-2001 simulation was used. Using the interpolated temperature and salinity

along the open boundary, the low frequency surface elevation gradient was inferred from the density field based on the thermal wind relation. This is the relation between geostrophic currents and horizontal density gradient (see e.g., Pedlosky, 1987), with a zero-velocity reference depth of 100 m or the ocean floor if it is shallower than 100m. The calculation of absolute sea surface elevation along the open boundary requires a reference point where the absolute sea surface elevation is known. The outer coast of Cape Cod was used as the reference point.

The transects of interpolated temperature, salinity, density and RMS (for overall quality of interpolation of temperature, salinity and density) along the open boundary in April and August are shown in Figures 2.5. The RMS estimates in April on the open boundary are lower than that of August because the station coverage in April is better than in August (Figures 2.4). Unlike normal years, the water column in April 2005 was clearly stratified in coastal areas due to freshwater runoff creating strong horizontal and vertical salinity gradients. In August, both surface heating and freshwater runoff produce a warm and fresh surface layer. Overall, the interpolated temperature and salinity distributions on the open boundary well represent the seasonal cycles of the water column stratification in the GOM throughout the year. However, short-term (days-weeks) variations are not resolved in these boundary forcing conditions due to inadequate spatial-temporal coverage of data. In addition, the cross-shelf density gradient near the northern coast, which represents the baroclinic component of the WMCC, may not be well characterized.

The estimated monthly surface elevations are shown in Figures 2.6. The horizontal gradients determine the long-term geostrophic currents into or out of the model domain. Note that the nearly flat elevation in January is caused by the absence of observations during that month. In spring and summer, the results indicate an overall inflow in the northern portion of the open boundary and a nearly permanent outflow in the southern portion of the open boundary. In late October-December, the interpolated results suggest a weak or reversed coastal current near the northern coast, which differed from results during normal years. The interpolated seasonal patterns of temperature, salinity and currents are consistent with other modeling results for the GOM region (Lynch et al., 1996; Xue et al., 2000).

As in previous simulations, the numerical schemes of boundary conditions for all scalars in the hydrodynamic model were radiation condition during out-going flow and relaxation to specified boundary values during in-coming flow, respectively (HydroQual and Signell, 2001;

Jiang and Zhou, 2004a). The tangential and vertical velocities along the open boundary were derived from values at the nearest interior grid-points (i.e., zero horizontal velocity gradients), whereas the normal velocities were allowed to change freely.

2.4.4 Assimilation of GoMOOS B measurements

Measurements at GoMOOS buoy B, which is close to the model northern open boundary, started in August, 2001. Temperature, salinity and currents measured at this location all show strong short-term variability that are naturally absent in the objectively interpolated open boundary conditions (Figures 2.5-2.6). The mooring station resides in the core of the WMCC and because the WMCC normally flows southwestward toward the MBS, the variability in these measurements represents the variability of upstream open boundary conditions. Incorporation of this information into the model should improve the model performance. Same as in the 2002-2004 simulations, the assimilation for 2005 is implemented on the first interior grid-line (I=67) of the model domain (Figure 2.1). Since the horizontal gradients of temperature, salinity and currents cannot be resolved by measurements at a single station, some subjective choices are used to extrapolate the single-station to a transect from the coast to approximately 20 km offshore. The data assimilation technique used is called nudging, which is essentially restoring model fields (temperature, salinity and currents in our case) to the values from observations with a specified time-lag (Eq. 2.4). In our case, we restore the model values to the final values of temperature, salinity, and currents along the 20 km cross-shelf transect.

At GoMOOS buoy B, temperature and salinity were measured at three depths (1m, 20m, 50m) (Figures 2.7). Measured temperature and salinity were first smoothed using a 25-hr running mean filter to remove high frequency signals and then linearly interpolated between measured depths to derive vertical profiles (referred to as observed values hereafter). These profiles were projected onto the closest interior grid point BB (I=67, J=58). To maximize the assimilation effect, the observed values were further projected horizontally over the grid-line, a cross-shelf transect between the coast (point C) and an offshore location (point D) (Figure 2.1). The projection for the segment C-BB was based on the observed values at BB and the modeled temperature and salinity gradients at BB (from previous time-step), while for the segment D-BB, the projection was based on the linear interpolation between modeled values at D (from previous time-step) and observed values at BB. In the simulations, the temperature and salinity between

C and D were restored to the final temperature and salinity values with a time-lag of t_{lag}=2 hour as follows (using temperature as an example),

$$\frac{dT}{dt} = \frac{T - T_{final}}{t_{lag}} \tag{2.4}$$

Similar assimilation was made for currents at GoMOOS buoy B, which were measured by an Aanderaa current meter (2m) and an Acoustic Doppler Current Profiler (ADCP) (10-54m) (Figure 2.8). Measured currents were first linearly interpolated into model sigma layers. Then all of the modeled currents at the grid-points between C and BB were restored to the interpolated current values with a time-lag of 1-hr, whereas currents at the grid-points between BB and D were restored to the interpolated current values with a time-lag increasing from 1-hr at BB to 8-hr at point D.

Numerical simulations were conducted by assimilating (1) temperature and salinity (TS) only and (2) both TS and currents. The results with the assimilation of only TS show significant improvements in modeled temperature and salinity, but somewhat decreases the quality of modeled bottom currents. Meanwhile the assimilation of both TS and currents improves modeled temperature, salinity and currents. All results presented below were from simulations assimilating both TS and currents.

2.4.5 Initial conditions

The initial conditions for the hydrodynamic model are derived from the modeled results in the end of 2004 simulation without spin-up.

Table 2.1 Prognostic model variables

Variables	Descriptions
el	surface elevation (m)
u & v	horizontal velocities (m/sec)
w	sigma coordinate vertical velocity (m/sec)
T	temperature (ºC)
S	salinity (psu)
rho	density (kg/m^3) (derived from T and S)
q2	twice the turbulent kinetic energy (m^2/sec^2)
q2l	q2 times turbulent length scale (m^3/sec^2)
l	turbulent length scale (m) (=q2l/q2)

Table 2.2 Key parameters of hydrodynamic model

Parameters	Values
Smagorinsky coefficient (horizontal mixing)	0.1
Bottom roughness	0.003 m
Vertical background mixing	$5x10^{-6}$ m^2/sec
Light attenuation coefficient	0.16~0.6 m^{-1}

Table 2.3 Frequencies and filtering of forcing data, validation data, and model output.

Parameters	Frequencies used in the model implementation or validation	Frequencies of original data	Filtering	Sources
Winds, air temperature, air pressure	hourly	hourly	no filtering in model input, 51-hr low-pass filtering in model-data comparison	NDBC 44013
Solar radiation	hourly	hourly	no	WHOI
Humidity	hourly	hourly	no	Logan Airport
Boundary temperature, salinity, elevation	monthly	various	Objective interpolation	NMFS, MWRA, UNH, SBNMS
River discharges	daily	daily	no	USGS
Outfall effluent flow	daily	daily	no	MWRA
Tidal forcing	every time step	N/A	N/A	ADCIRC
GoMOOS buoy A&B (T, S, currents)	hourly	hourly	25-hour running mean for T&S Lanczos filter (25-hour cut-off frequency) for currents	University of Maine
USGS buoy A (T, S, currents)	hourly	hourly	Lanczos filters with 25-hour cut-off frequency	USGS
MWRA Outfall Monitoring (T and S)	12 cruises for nearfield 6 cruises for farfield	12 cruises for nearfield 6 cruises for farfield	no	MWRA
Model output: time series (T, S, currents)	hourly	207 sec	Lanczos filter with 25-hour cut-off frequency	UMB
Model output: snap shots	Averages over one M_2 tidal cycle	207 sec	no	UMB

Table 2.4 Quality of data coverage for objective interpolation

Month	**Rating***
January	0
February	0
March	-
April	0
May	+
June	+
July	0
August	0
September	+
October	0
November	+
December	-

* Definitions of symbols: + (good), 0 (fair) and - (poor).

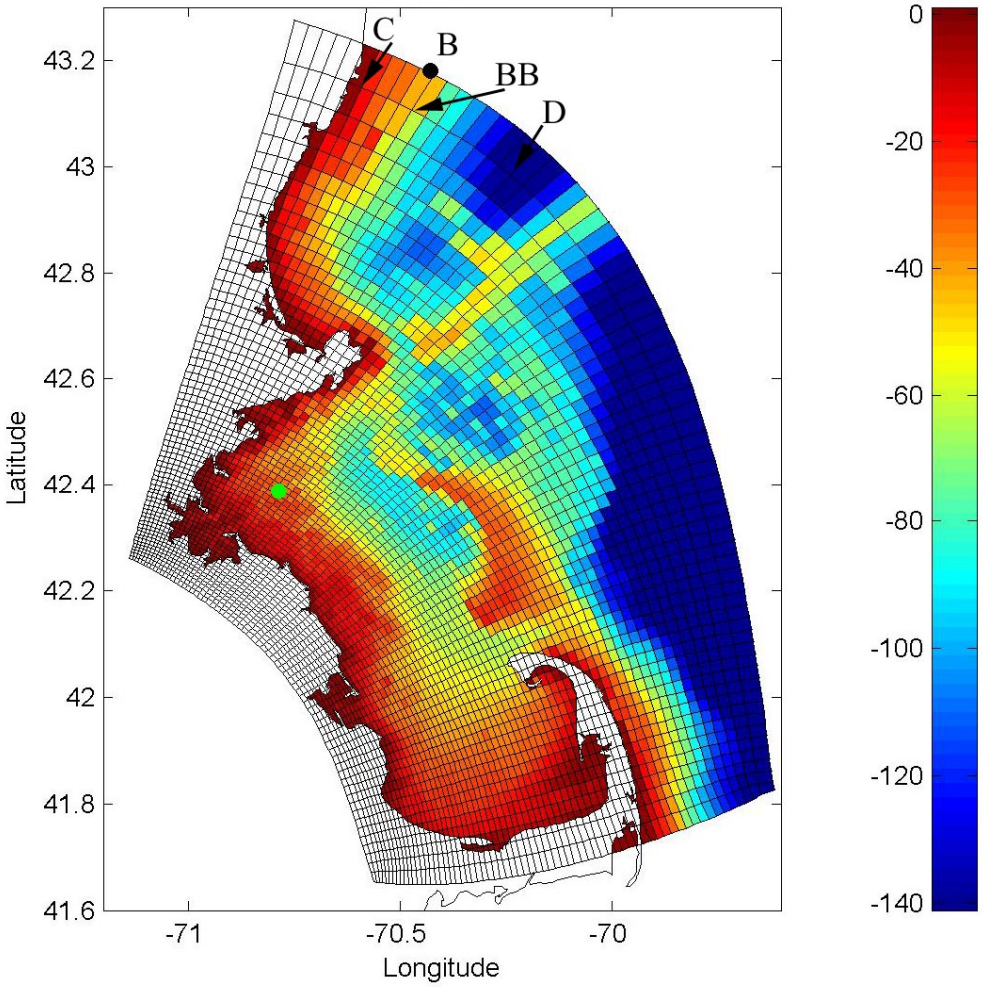

Figure 2.1. Model domain and grids in the MBS. Also shown are GoMOOS buoy B (black dot) and the MWRA outfall (green dot). Points C, BB, and D are reference points for data assimilation (see text).

(a)

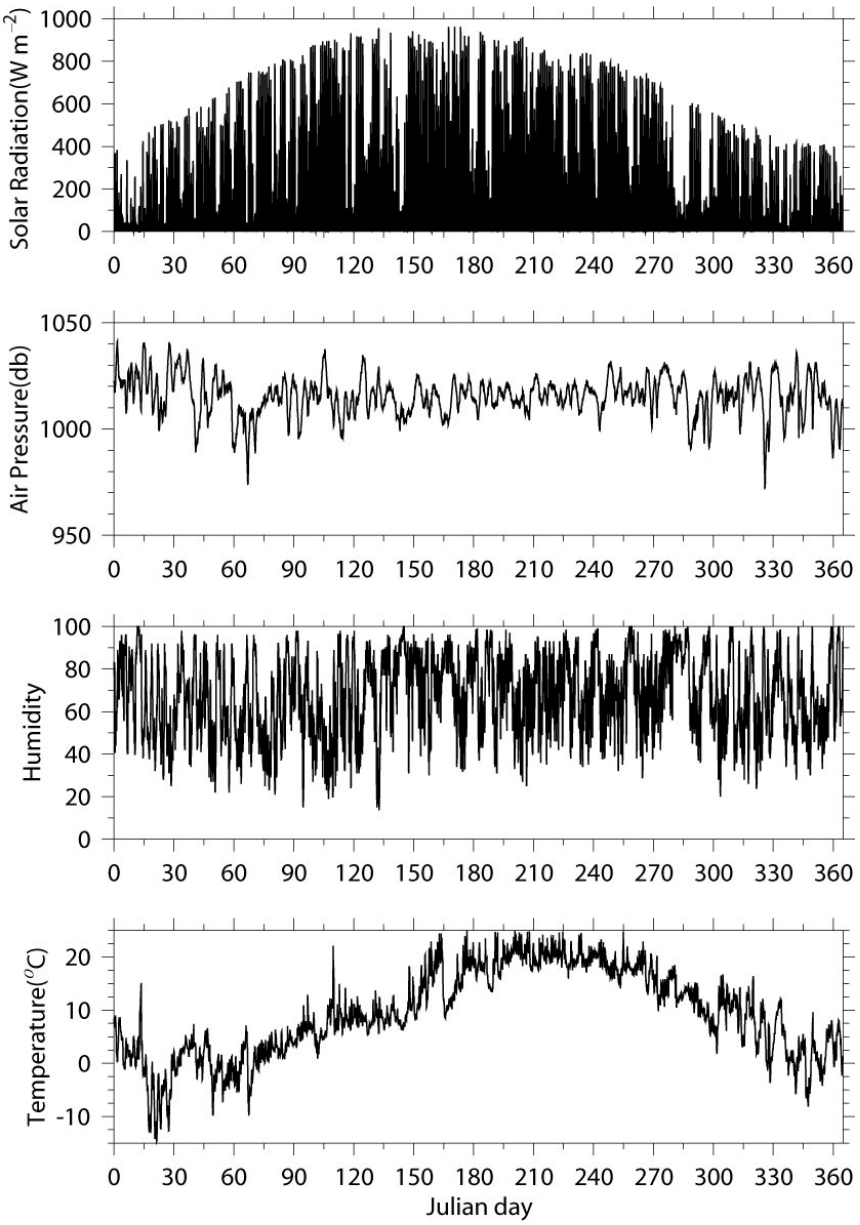

Figure 2.2 Meteorological forcing: (a) solar radiation, air pressure, humidity, and air temperature, and (b) wind speed and directions.

(b)

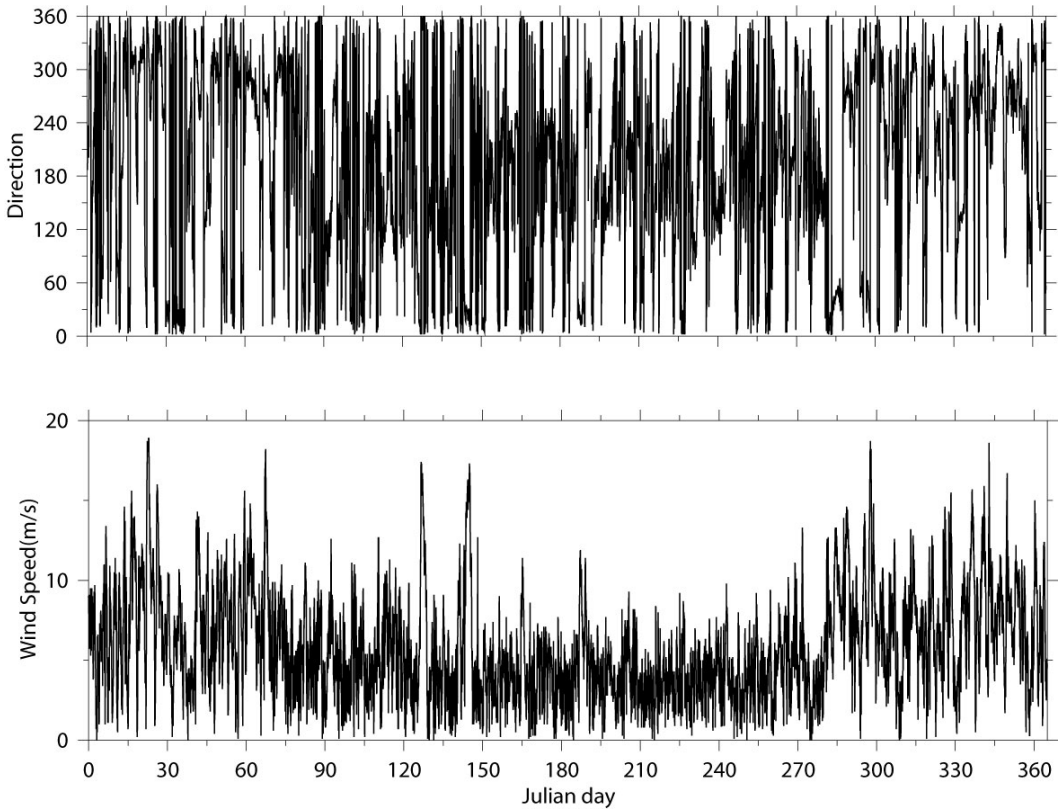

Figure 2.2. Continued.

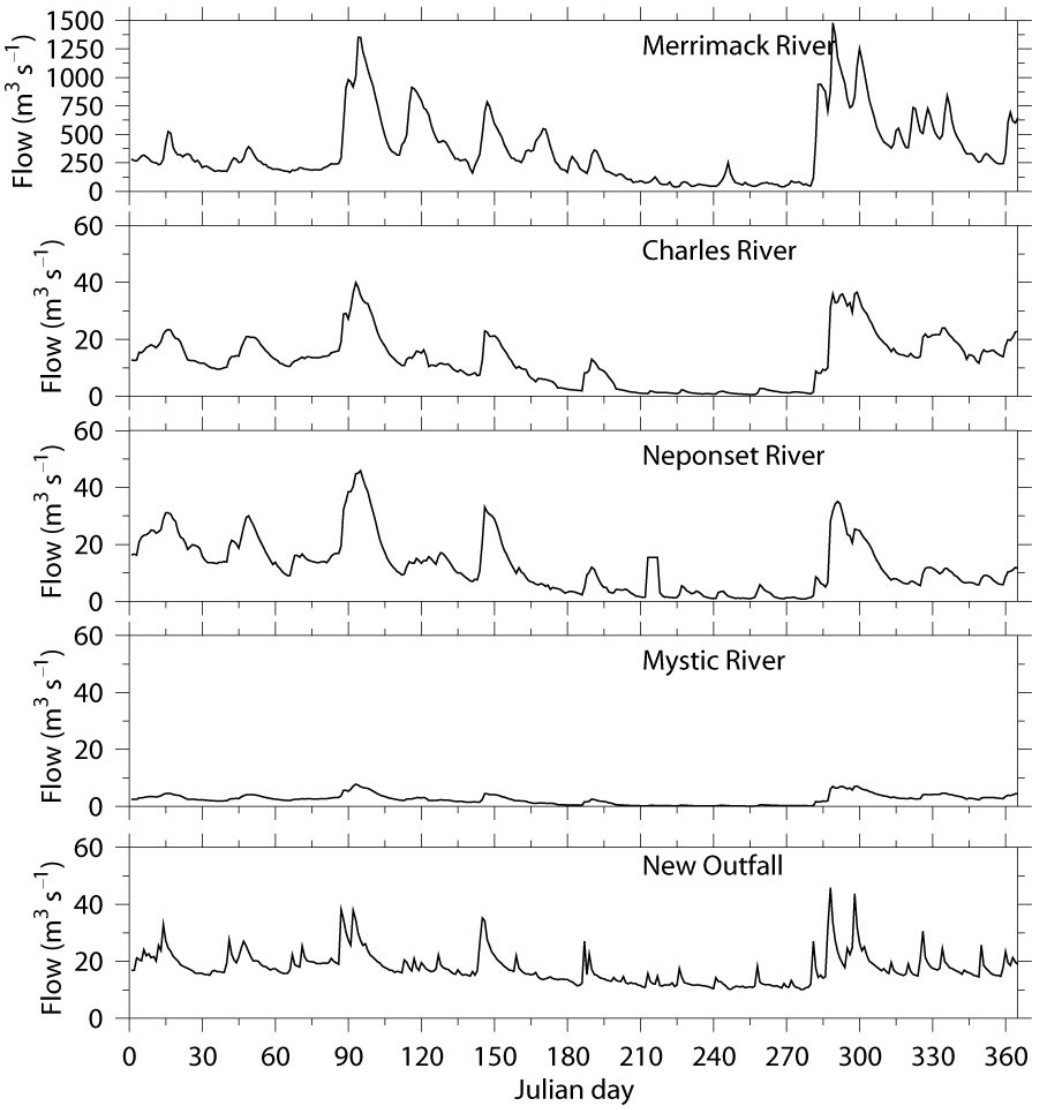

Figure 2.3 Daily discharges from the Merrimack River, Charles River, Neponset River, Mystic River, and MWRA outfall.

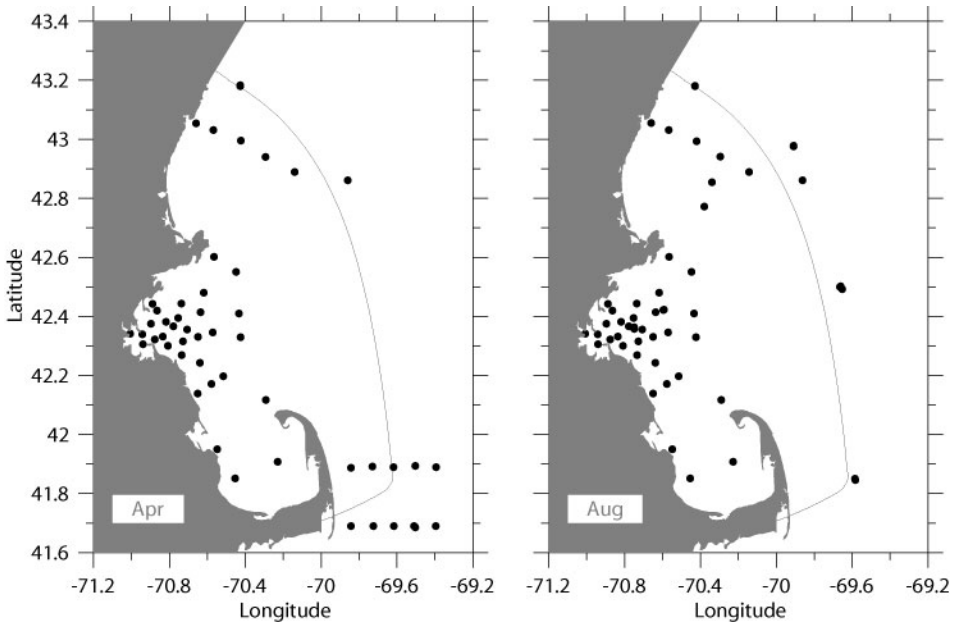

Figure 2.4 Station maps of available data in April and August.

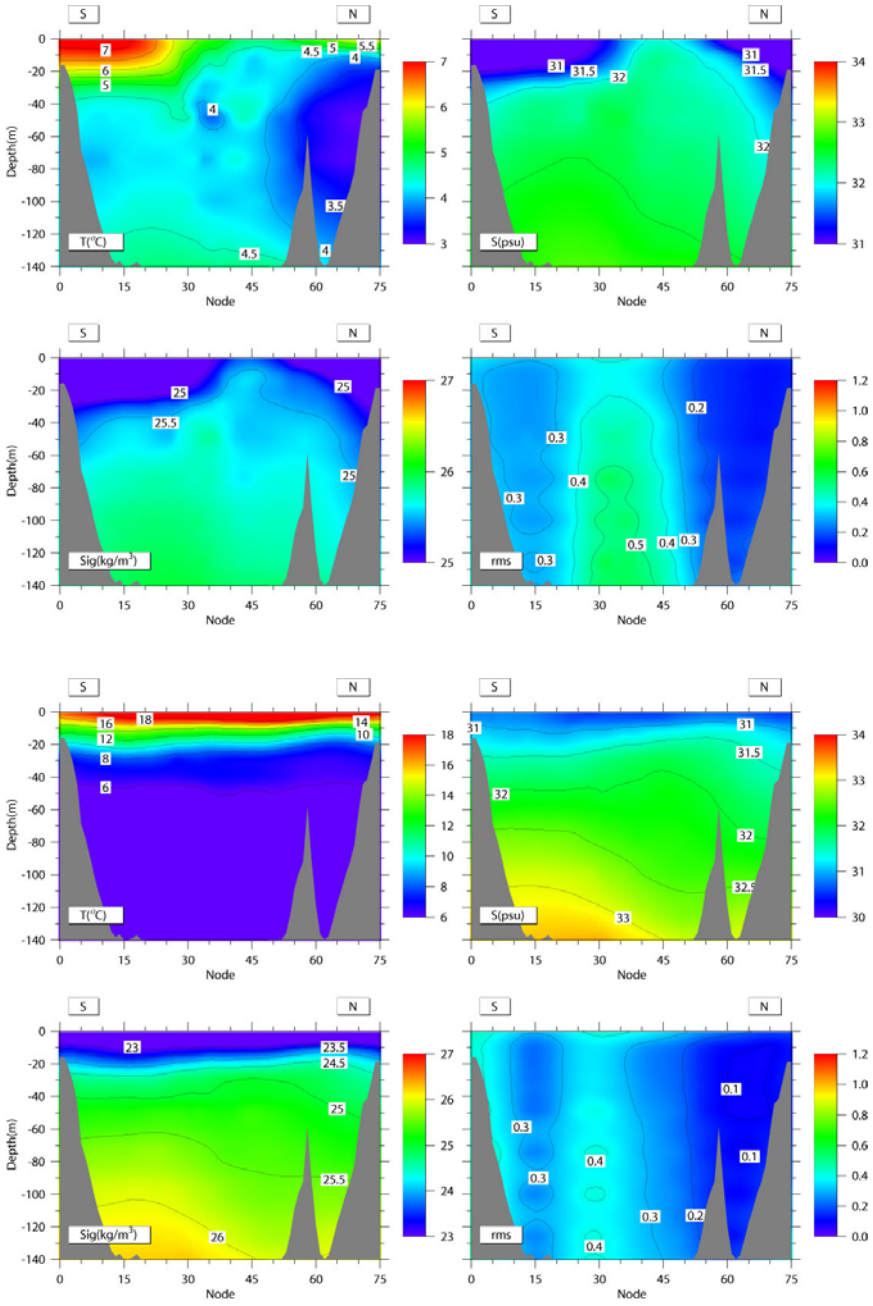

Figure 2.5 Open boundary conditions of temperature, salinity, σ_t and rms errors in (a) April and (b) August.

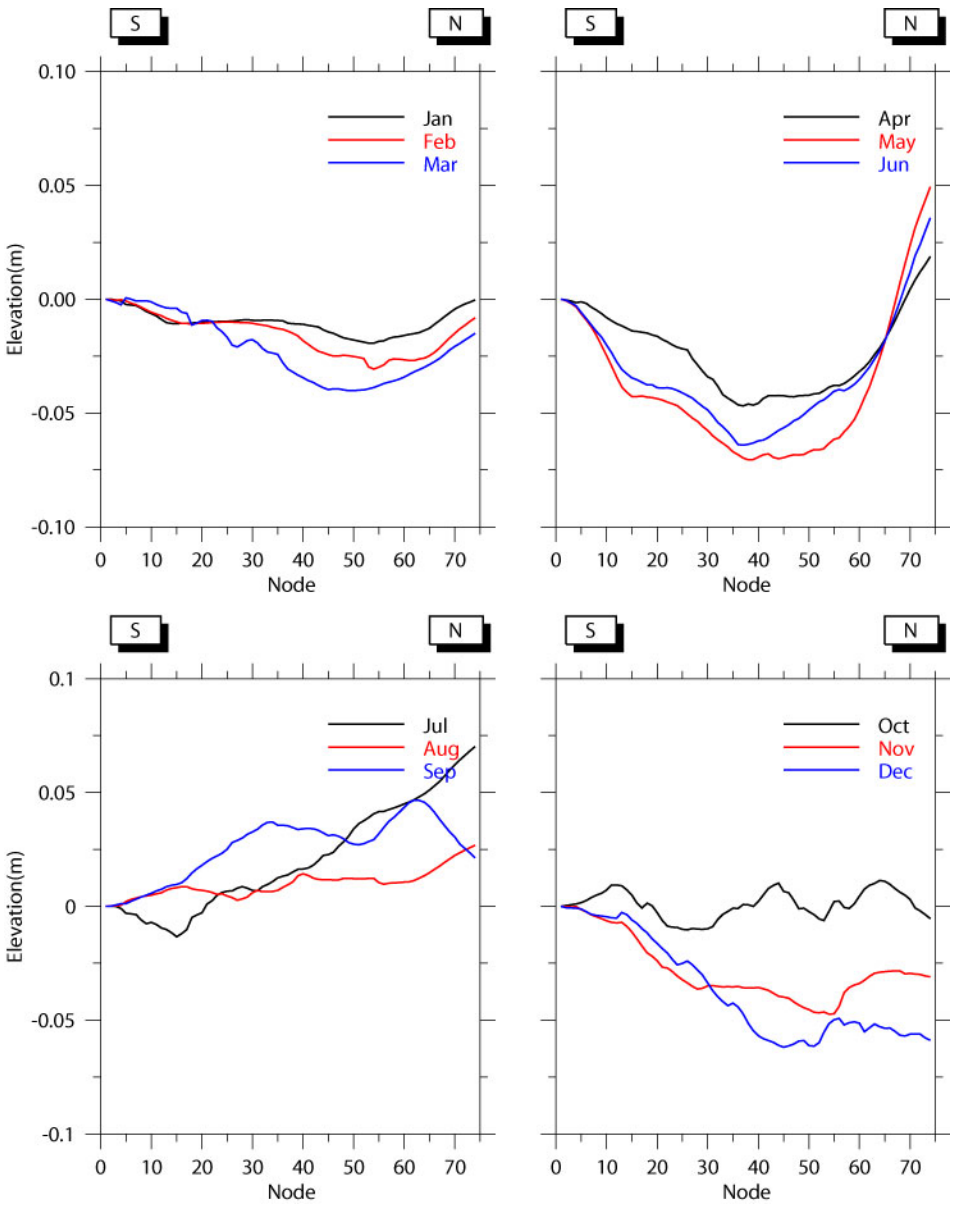

Figure 2.6 Monthly sea surface elevations at the open boundary.

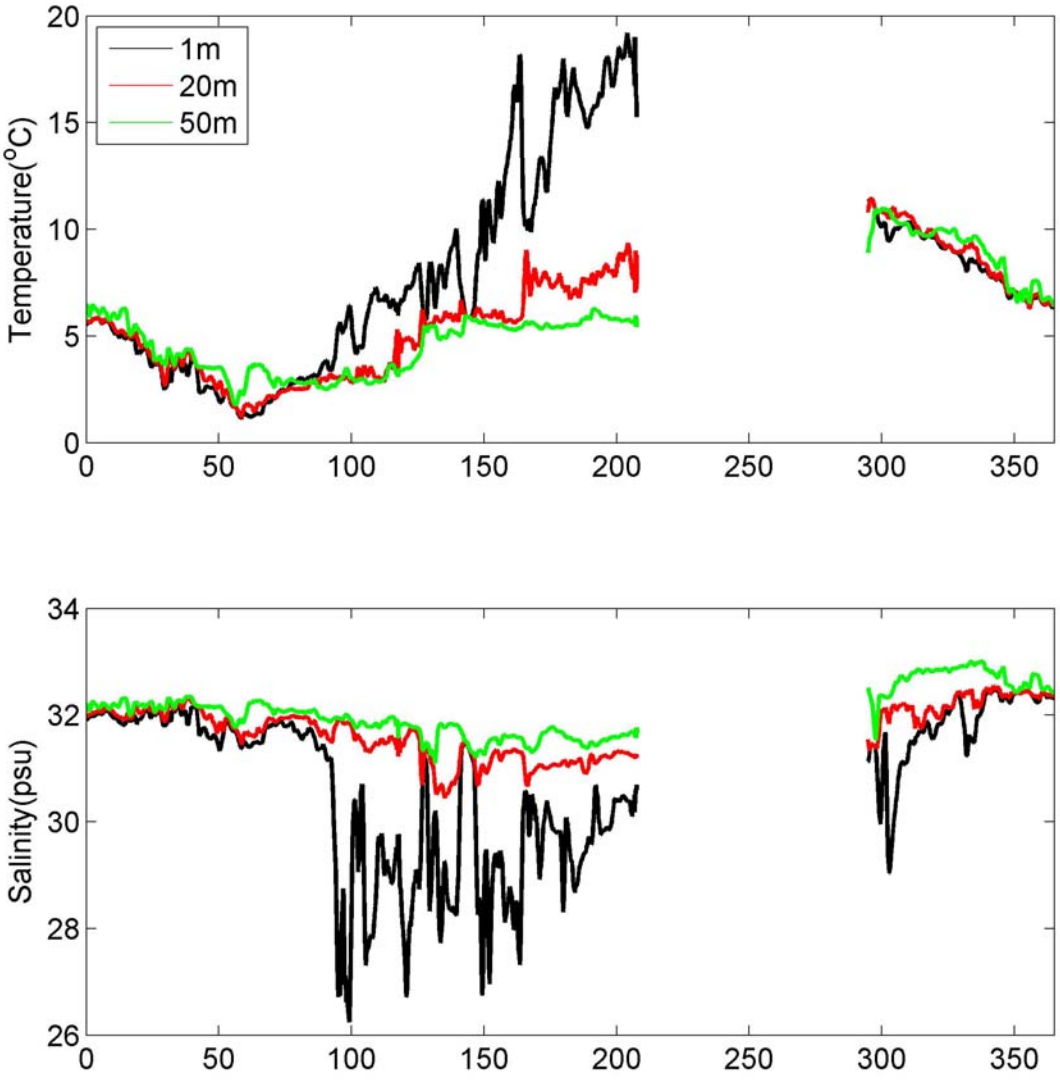

Figure 2.7. Temperature and salinity at GoMOOS Buoy B.

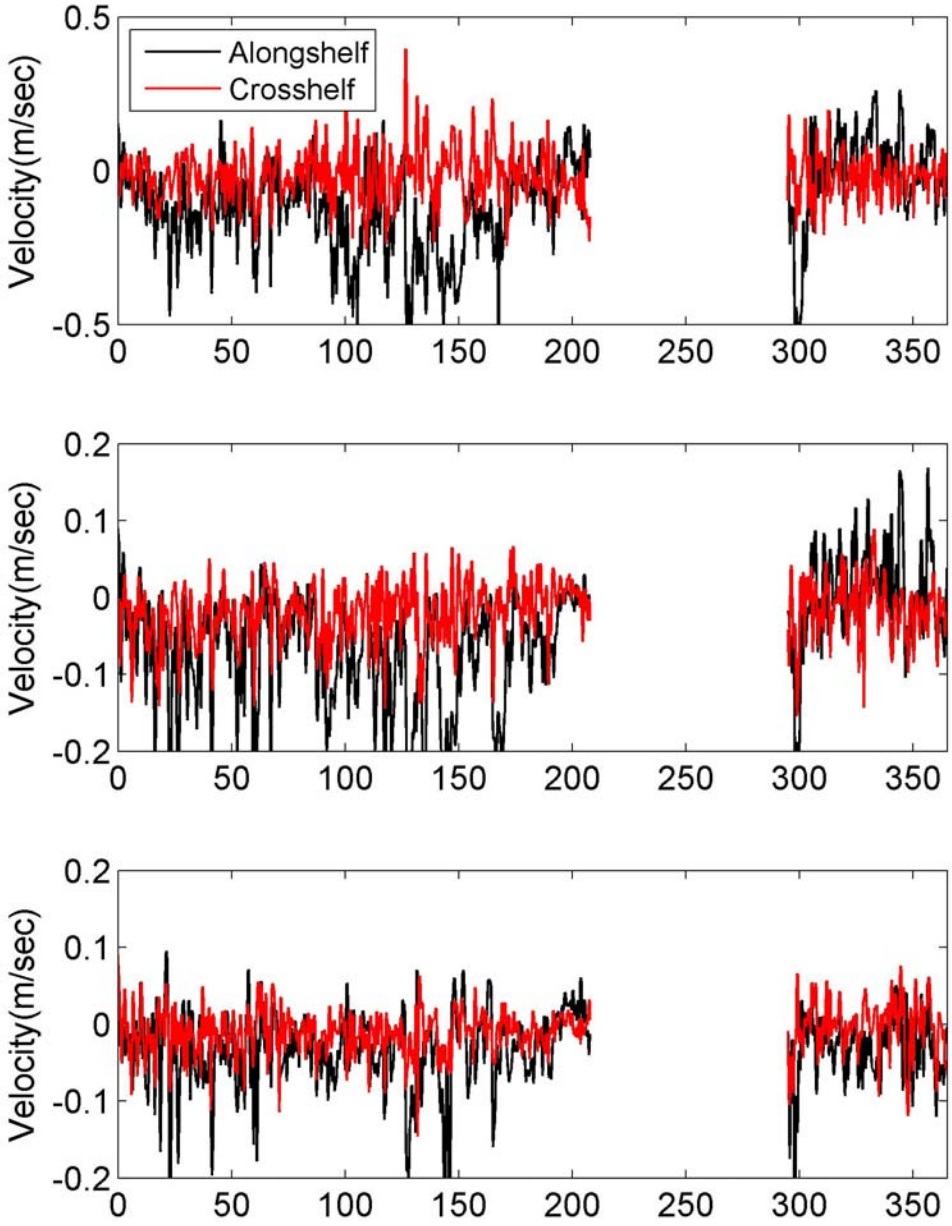

Figure 2.8. Along shelf and cross shelf currents at GoMOOS Buoy B (Top panel: 1m, middle panel: 20m, bottom panel: 50m). Measured currents were rotated counterclockwise approximately 60º.

3. MODEL VALIDATION AND DISCUSSION

This section will validate the numerical simulation by comparing model results with measurements of temperature, salinity and currents at mooring stations and from monitoring surveys. It will also discuss and highlight major hydrodynamic processes and events that occurred during the year.

3.1 Time series

3.1.1 Temperature and salinity

Twelve stations from the MWRA monitoring network were chosen for the data comparison (Figure 3.1). These stations are organized into four groups: a) stations F26, F27 and F29 along the eastern boundary of the MBS, b) stations F31, N01 and N10 in the coastal area of the northwestern MBS, c) stations F07, F01 and F02 in the southern MBS, and d) stations N04, N07 and F17 in the offshore region of the northern MBS. In the discussion, measurements at surface and bottom were compared with modeled results taken at the 1^{st} and 12^{th} sigma levels, respectively (Figure 3.2).

Modeled results were also compared with observed temperature and salinity at USGS buoy A (Figure 3.3) and GoMOOS buoy A (Figure 3.4). At USGS buoy A, no surface measurement was available for comparison. We used 10m and bottom measurements for comparison and corresponding to these depths, the model sigma layers were chosen as k=5 and k=12. At GoMOOS buoy A, the temperature and salinity measurements at the surface (1m) and near the bottom (50m) were compared with model results at the model 1^{st} and 10^{th} sigma layers, respectively.

The model well simulates the seasonal cycles and overall values of observed temperature and salinity (Figures 3.2-3.4). In particular, the model captured the strengths and timings of stratification in summer and de-stratification in fall. It also reproduced major events including a cooling event in January-February, summer upwelling and downwelling and the freshening events in both spring (April-June) and fall (October).

In winter, waters were relatively cold with temperature reaching zero in shallow area and about 2ºC in most of the bay during February and early March. Both local vertical heat fluxes and lateral heat transport contributed to the temperature field in the MBS. In winter, salinity was

at around 31.5, the highest in the year.

In spring, strong freshwater discharges occurred prior to two strong Nor'easters in May, which produced strong coastal currents and freshwater intrusions into the MBS from the GOM coast. The freshwater runoff events started in April and continued into June. Surface salinities reached their minima in April and then varied during these three months. This variation was due to horizontal transport of coastal fresh and oceanic waters associated with currents and mesoscale eddies, and vertical mixing between surface and bottom waters (Figures 3.4-3.5).

In May, two strong Nor'easters produced strong westward Ekman transport pushing offshore waters against the coast and driving very strong coastal currents. The winds also produced strong vertical mixing that destratified the water column at stations shallower than 40m (Figures 3.3-3.4). The model predicted both mixing events.

In mid–June, a warming event was observed at some stations (F27, N01, F17), consistent with observations at GoMOOS Buoy A (Figure 3.3) and Buoy B (Figure 2.7). This event was reflected in the model surface temperatures at those stations though the modeled temperature was lower than the observed. The warming was related to a coastal warming event due to an atmospheric heat wave hitting the region (Figure 2.2).

During summer, the model run reproduced the strong temperature and salinity oscillations in near-shore areas which were associated with coastal upwelling and downwelling winds. Such oscillations were observed at USGS buoy B off Scituate in previous studies (Jiang and Zhou, 2006).

In fall, surface cooling and vertical mixing events in the MBS were well simulated in the model runs. Waters in shallow coastal areas were cold and well-mixed. The strong fall river discharge started from mid-October and lasted for about one month, which was not present in normal years. Similar strong river discharges were observed in the rivers throughout the GOM region. It appeared that most of the freshwater from the Merrimack River and upstream in the GOM bypassed the MBS along the outer edge of the Stellwagen Bank. The event produced a decrease of both surface and bottom salinities in the MBS. The model reproduced this freshening event though the salinities were underestimated at some inshore stations.

3.1.2 Currents

Currents were only measured at the two available buoys (USGS buoy A and GoMOOS buoy A). Similar to the temperature and salinity comparison, the 10m and bottom currents at USGS buoy A were compared to surface and bottom currents at GoMOOS buoy A (Figures 3.5–3.12).

In spring (April–June), the model predicted current directions and magnitudes well at both mooring stations (Figures 3.6 and 3.10). In particular, the model predicted the strong coastal currents at GoMOOS Buoy A during the spring flooding and the two Nor'easters (Figure 3.10). However, at the USGS buoy A the model predicted a southwestward flow at 10 m between April 15 and May 1, while observed currents were in the opposite. At this location, the model also predicted a strong mid-depth southwestward flow in June when the observations indicate a weaker current.

In summer, the model had difficulties predicting observed currents, especially bottom currents (Figure 3.11). These difficulties were also encountered in our previous simulations (Jiang and Zhou, 2004c, 2006b). The discrepancies in short-term variability between modeled and observed currents, especially bottom currents, at GoMOOS buoy A may indicate the uncertainty in predicting the currents and bifurcation around Cape Ann, which results from interaction between local surface winds, topography, freshwater plume and the WMCC. The smoothed open boundary conditions and bottom topography can certainly contribute to the uncertainty.

During the winter and fall (January-March and October-December), the model was able to predict surface, mid-depth and bottom currents at both mooring stations (Figures 3.5, 3.8, 3.9 and 3.12). During this period, surface and 10m currents were mainly driven by surface winds, which led to strong correlations between winds and currents from both model and measurements. There was no indication that unusually strong freshwater inputs from rivers around the GOM during this period had enhanced the WMCC. However, the bottom currents were less coherent with surface winds during the winter and fall. A strong northwestward flow existed at both mooring stations during October–December which was predicted by the model though the magnitude was overestimated (Figures 3.8 and 3.12).

3.2 Spatial patterns

The hydrographic surveys in the MBS typically took 2-4 days. To make the comparison with observed data, modeled temperature and salinity data were averaged over one semidiurnal tidal period centered on each survey period. Daily sea surface temperature (SST) data acquired by the Moderate Resolution Imaging Spectroradiometer (MODIS) were also used for comparison (Data was courtesy of A. Thomas, University of Maine). Similar to the time series comparison, the spatial comparison is to assess the model capability and quality in predicting spatial variability. Overall, the model was able to reproduce spatial patterns observed. To elucidate the comparison, several specific events were presented such as winter cooling and mixing, spring freshwater plume from the Merrimack River and other upstream rivers, and coastal Ekman transport associated with Nor'easters (Figures 3.13–3.15).

3.2.1 Winter cooling and mixing

In winter, strong northwesterly winds and surface cooling produced cold waters and strong vertical mixing in the MBS. Waters in shallow coastal areas were cold and well-mixed. A strong temperature front was located about 30–40 km from the coast separating the colder coastal water from warmer oceanic waters from the western GOM as evident in both the satellite image and model results on March 14, 2005 (Figure 3.13). The front also defines the main path of the WMCC. The model temperature was about 1ºC lower than that from the satellite. Since the satellite estimated SST data have not been calibrated using *in situ* data, we will not be able to conclude the significance of the temperature discrepancy. Regardless, the similarity between modeled and MODIS SST distributions implies that the model has presented the most dominant processes driving the spatial variability.

3.2.2 Freshwater plume in spring

The WMCC is driven by wind stress and freshwater inputs from local rivers around the GOM. In spring and early summer, freshwater discharges from local rivers in the GOM determine the salinity, location and structure of the WMCC. Near Cape Ann, the largest freshwater source for the WMCC is from the Merrimack River. When the WMCC bifurcates, the freshwater from the Merrimack River and other rivers upstream intrudes into the MBS along with nutrients and biota. It is important for the model to be able to accurately simulate the path

and area coverage of the freshwater plume.

In 2005, the spring freshet started at the end of March, earlier than normal years and with a record high discharge (Figure 2.3). However, winds were either weak or northwestward during the first several days in April, as the currents south of Cape Ann were weak (Figure 3.10). As a result, the majority of freshwater from the Merrimack River was limited to northeast of Cape Ann (not shown). Model results suggest that the freshwater plume moved into MB around Cape Ann by April 5 and reached Marblehead on April 7 (Figure 3.14). Model results also suggested that during this time, most of the freshwaters in MB were from the Merrimack River. The model results are consistent with data collected during that period.

Two Nor'easters occurred in May 2005. The first storm arrived in the region after a month-long high river discharges in the region. Strong Ekman transport driven by northerly winds pushed surface waters into the MBS and led to strong coastal currents. The large amount of freshwater transported into the MBS lowered the overall salinity in the bays. Two days after the storm, the surface salinity in the majority of the MBS was lower than 30 (Figure 3.15). The spatial pattern of modeled surface salinity agreed with the pattern from data collected during the field survey. In particular, both model and data suggested that an anti-cyclonic eddy formed south of Cape Ann with a radius of about 10 km and current speed of about 20cm/sec. In addition, a salinity front was found separating the MBS waters and GOM intruding waters. Modeled salinity, however, was about 0.5 lower than the observed, which suggested that the model might have over-estimated the freshwater influx from the GOM.

Similarly, the second Nor'easter, which lasted longer than the first storm, produced a strong Ekman transport of the GOM surface water into the MBS, and led to strong coastal currents in the MBS. Modeled surface salinity agreed well with data collected between May 28 and 29 in both values and the patterns (Figure 3.16).

3.3 Impacts of the two Nor'easters in May 2005

The detailed time series of surface wind stresses at NOAA 44013, Merrimack River flow and surface temperature, salinity, currents at GoMOOS buoy A are shown in Figure 3.17. Before the first storm, the salinity in the MBS had already decreased dramatically from its winter values due to river discharges in April. A large freshwater plume carried the freshwater from both the

Merrimack River and New Hampshire coastal runoffs and penetrated deeply into the MBS (Figure 3.18).

As stated in the previous section, the strong northerly winds from the first storm produced a strong onshore Ekman transport that pushed salty oceanic waters into the MBS and created a strong coastal current (Figures 3.17 and 3.19). When the winds relaxed, the strong coastal current became unstable on May 10, and an anti-cyclonic eddy was formed south of Cape Ann with a radius of 10km with a current speed of about 25 cm/sec which was evident in both the model and survey results (Figures 3.15 and 3.20). The eddy brought salty oceanic waters with rich nutrients toward the north shore area. The western edge of the eddy was in contact with the MWRA outfall. Therefore, it might also have brought effluent nutrients toward the north shore area. A nested high resolution modeling study suggested that the eddy moved southwest toward the western coast and lasted for about a week.

The second storm produced similar onshore Ekman transport, strong coastal currents, and a significant increase in salinity during the storms. However, surface salinity in the MBS decreased significantly after the storm because of the high runoff from the Merrimack River produced by the heavy precipitation brought with the storm (Figure 3.17).

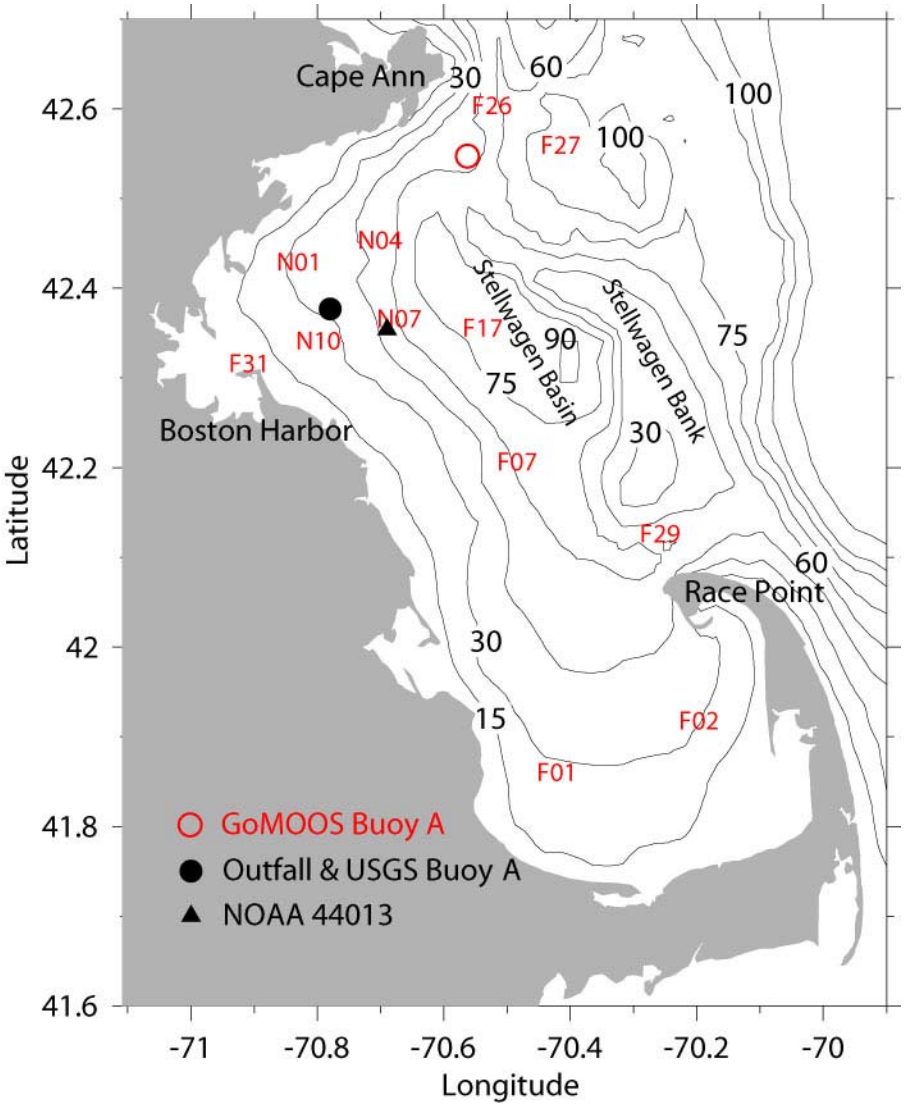

Figure 3.1. Stations used for the model validation.

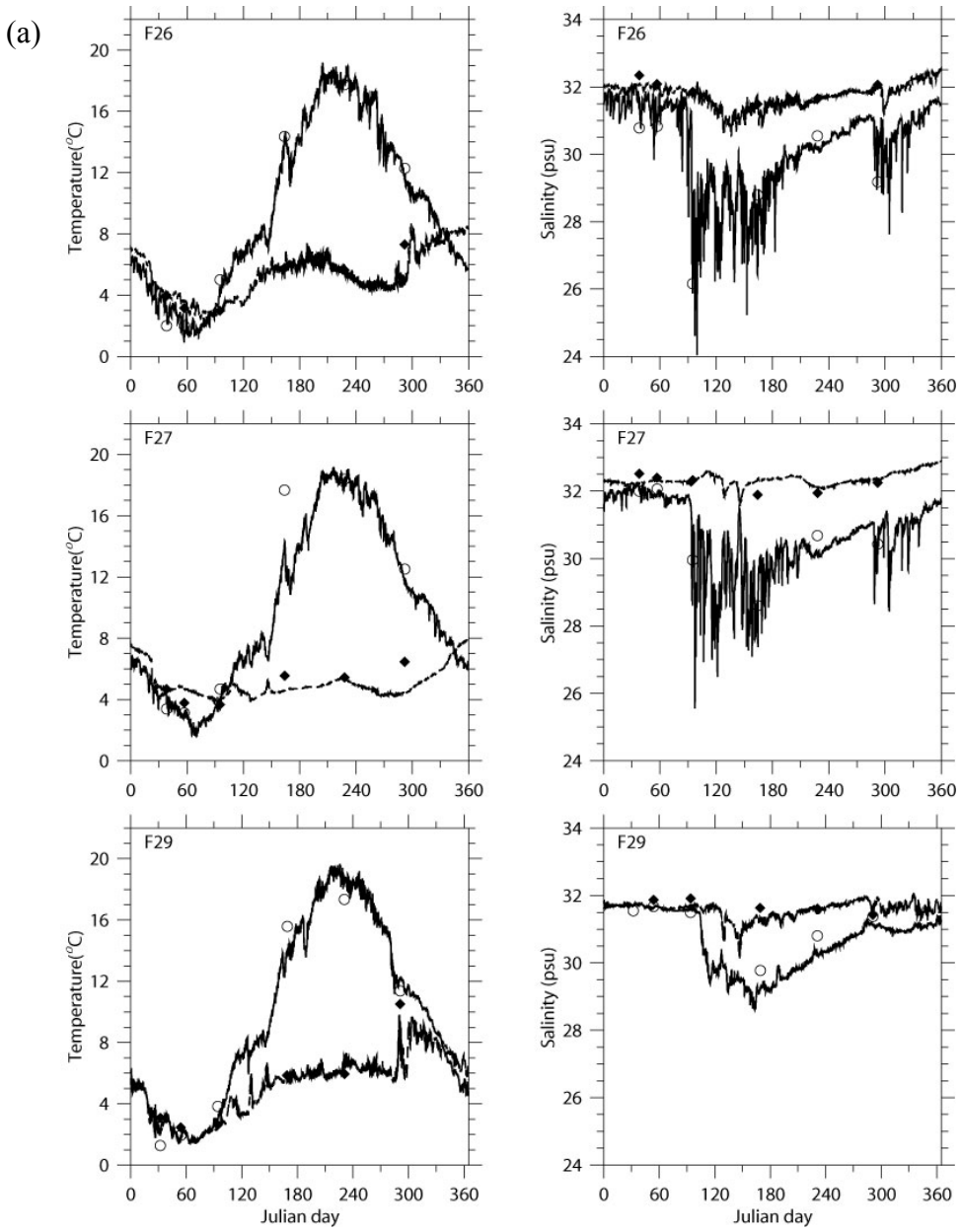

Figure 3.2. Modeled and observed temperature and salinity at selected stations.

(b)

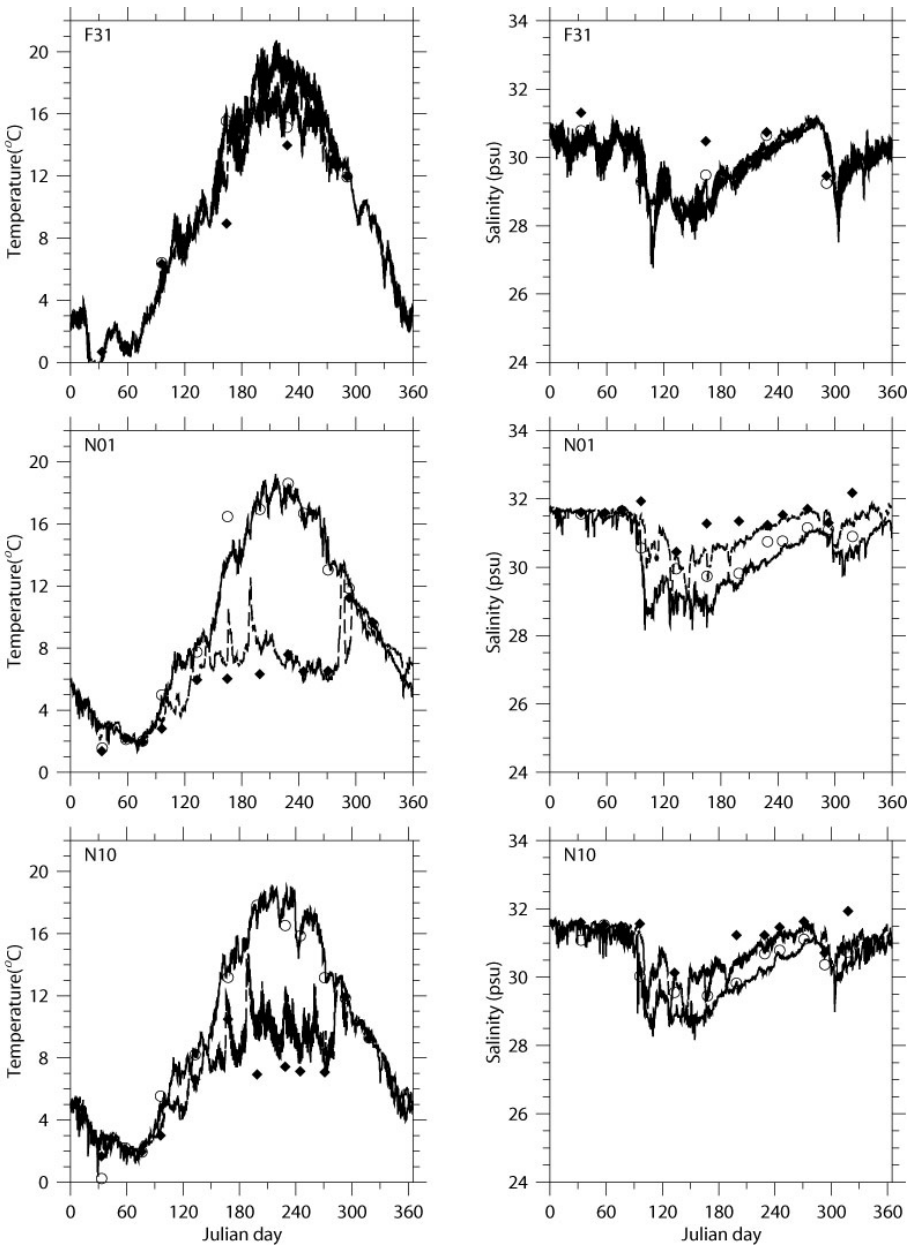

Figure 3.2. Continued.

(c)

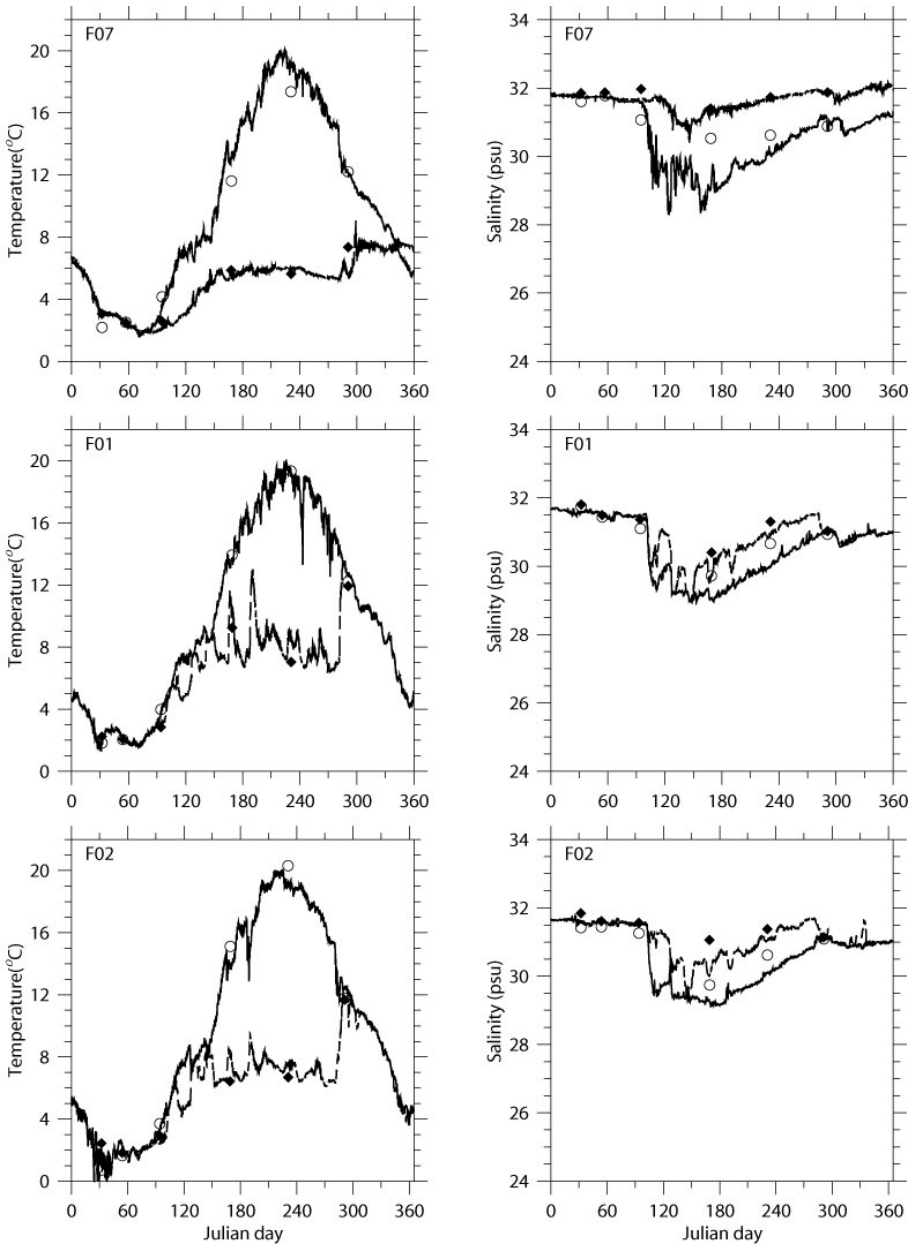

Figure 3.2. Continued.

(d)

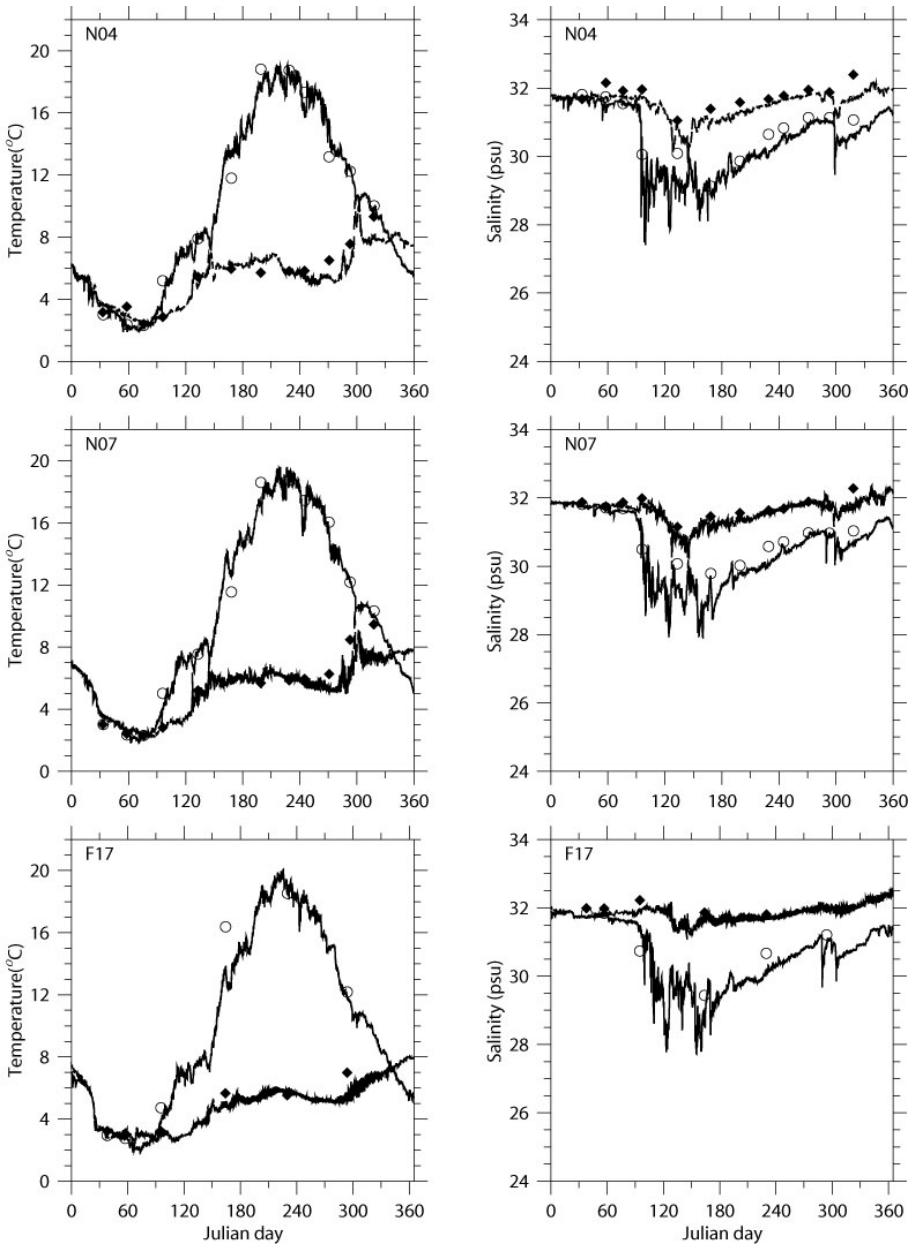

Figure 3.2. Continued.

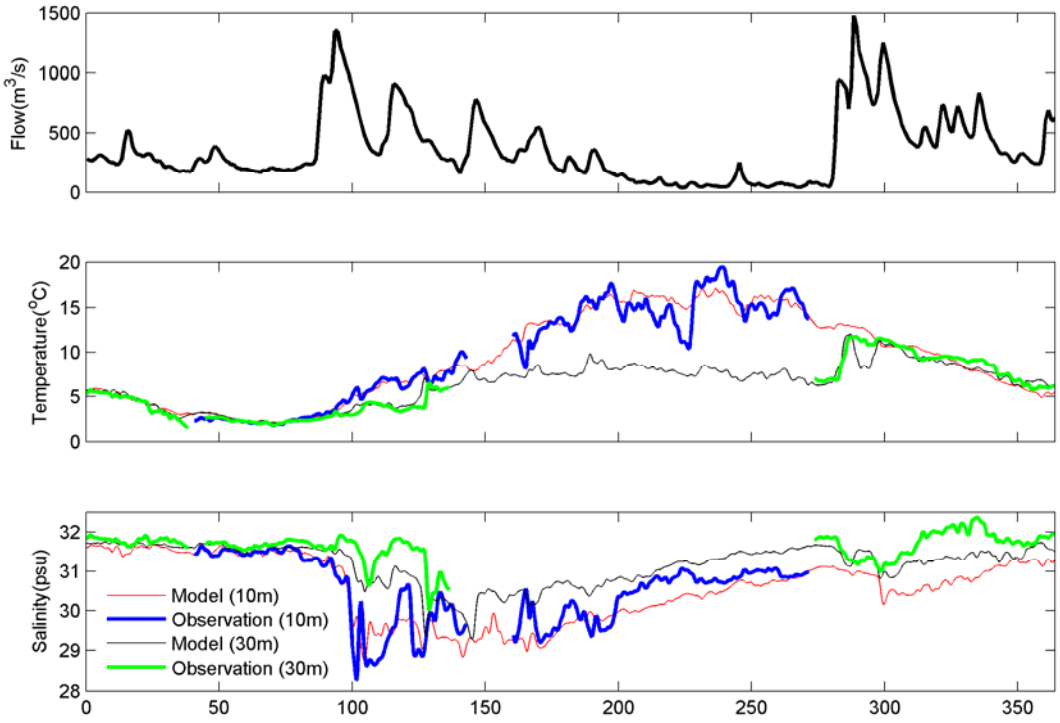

Figure 3.3. Merrimack River flow, and modeled and observed temperature and salinity at USGS Buoy A.

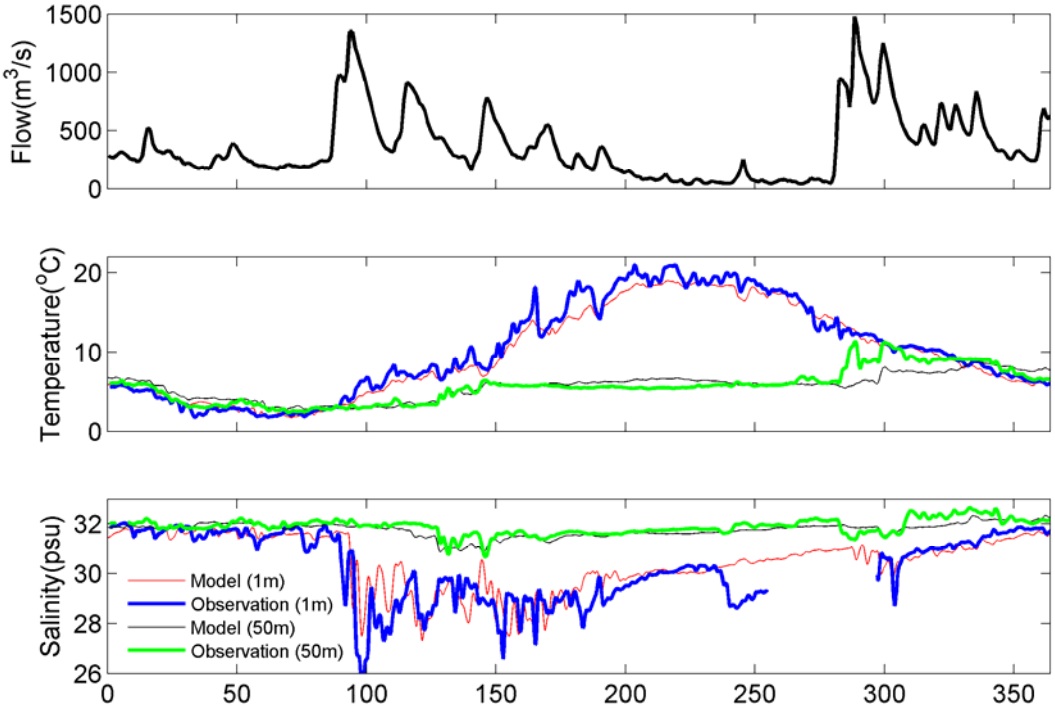

Figure 3.4. Merrimack River flow, and modeled and observed temperature and salinity at GoMOOS Buoy A.

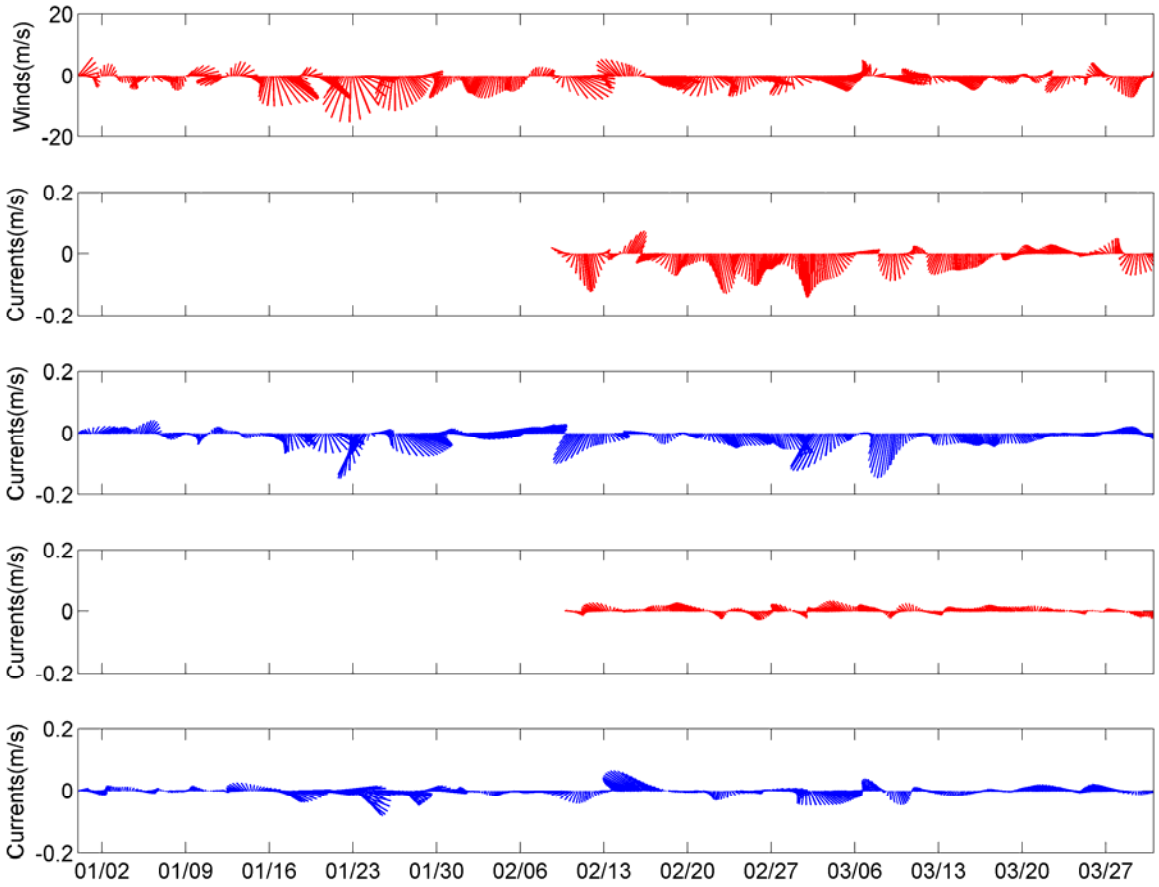

Figure 3.5. Winds at NOAA 44013 and currents at USGS Buoy A in Jan.-Mar. From top to bottom panels: Winds, observed currents at 10m, modeled currents at 10m, observed currents near bottom, and modeled currents near bottom.

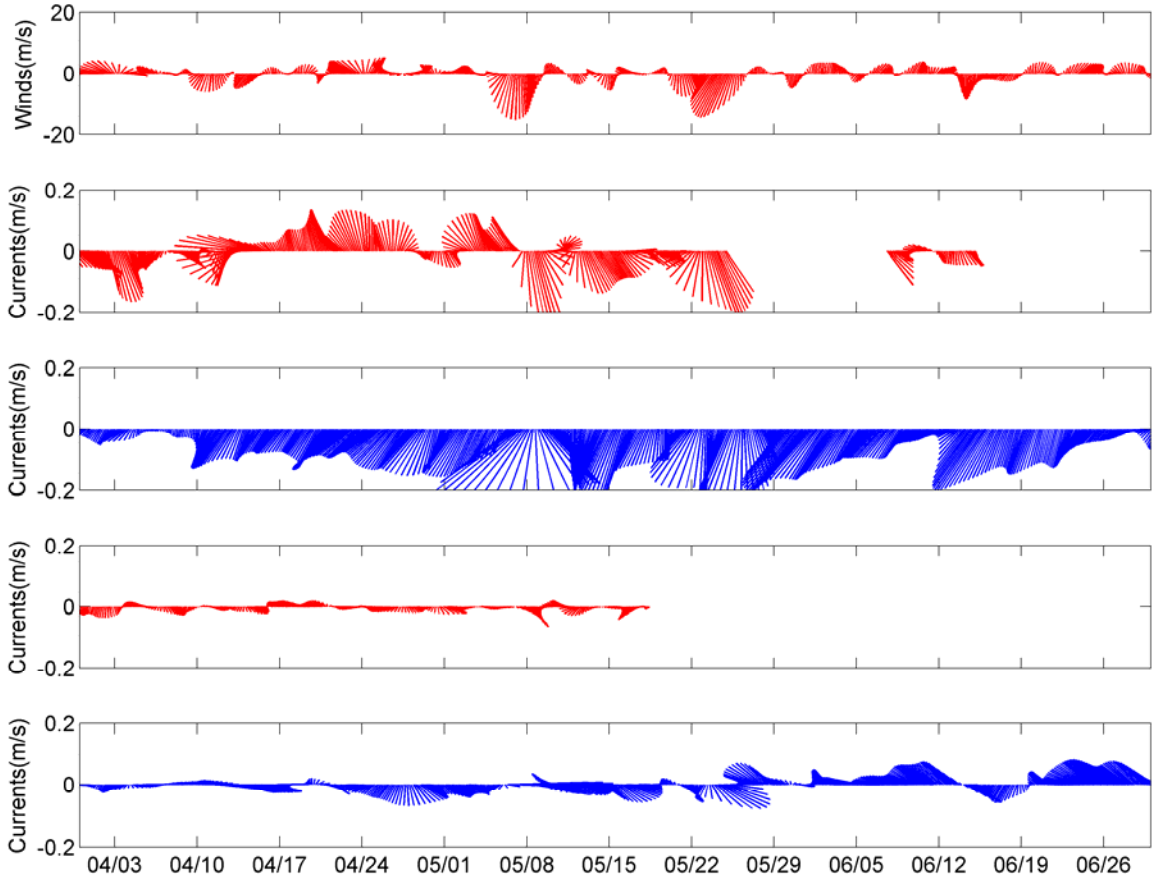

Figure 3.6. Winds at NOAA 44013 and currents at USGS Buoy A in Apr.-Jun. From top to bottom panels: Winds, observed currents at 10m, modeled currents at 10m, observed currents near bottom, and modeled currents near bottom.

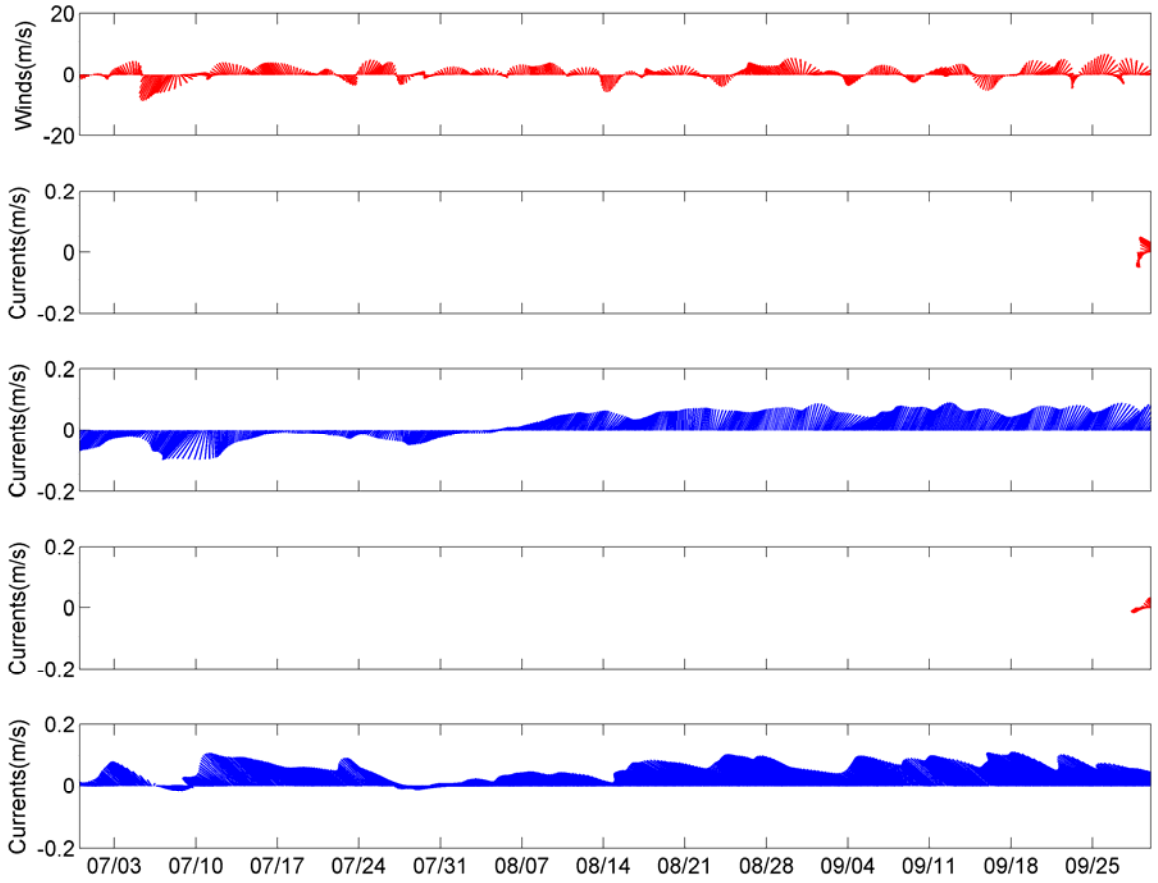

Figure 3.7. Winds at NOAA 44013 and currents at USGS Buoy A in Jul.-Sep. From top to bottom panels: Winds, observed currents at 10m, modeled currents at 10m, observed currents near bottom, and modeled currents near bottom.

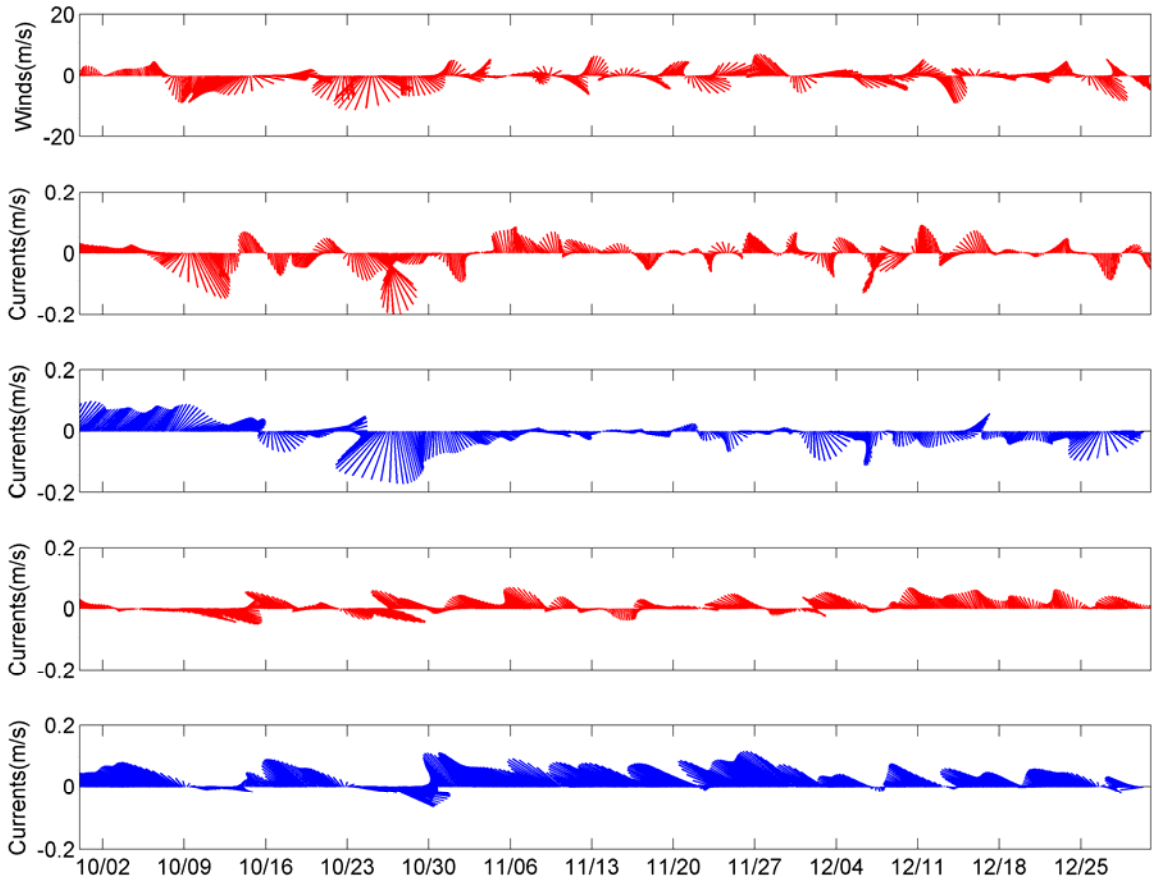

Figure 3.8. Winds at NOAA 44013 and currents at USGS Buoy A in Oct.-Dec. From top to bottom panels: Winds, observed currents at 10m, modeled currents at 10m, observed currents near bottom, and modeled currents near bottom.

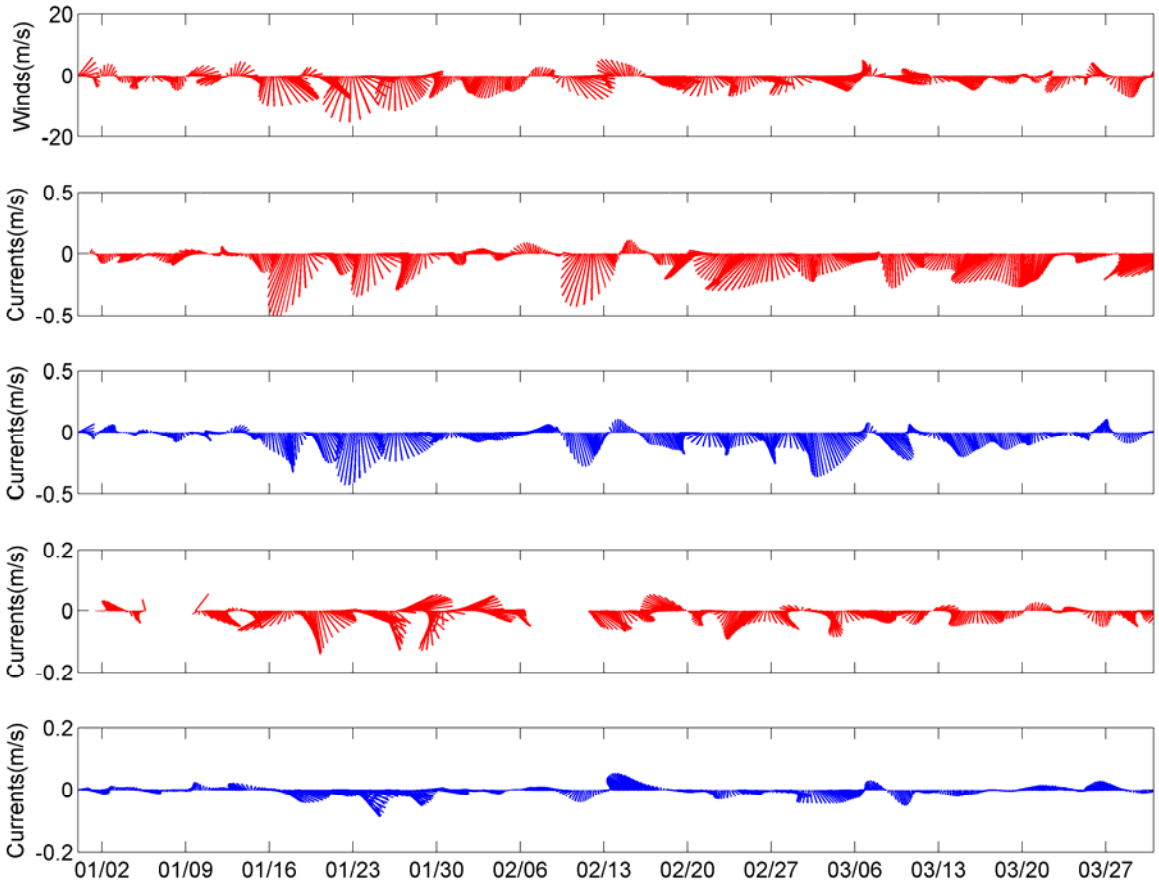

Figure 3.9. Winds at NOAA 44013 and currents at GoMOOS A in Jan.-Mar. From top to bottom panels: Winds, observed surface currents, modeled surface currents, observed currents at 50m, and modeled currents at 50m.

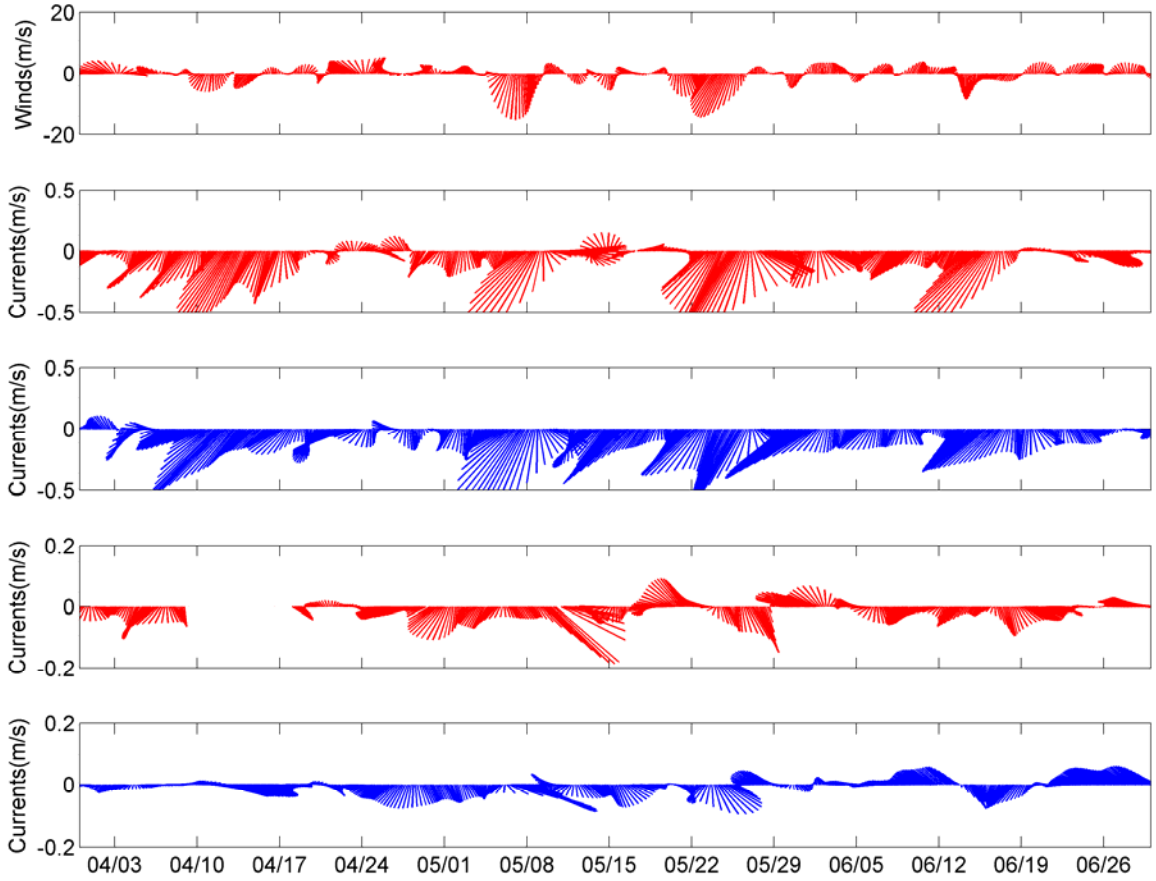

Figure 3.10. Winds at NOAA 44013 and currents at GoMOOS A in Apr.-Jun. From top to bottom panels: Winds, observed surface currents, modeled surface currents, observed currents at 50m, and modeled currents at 50m.

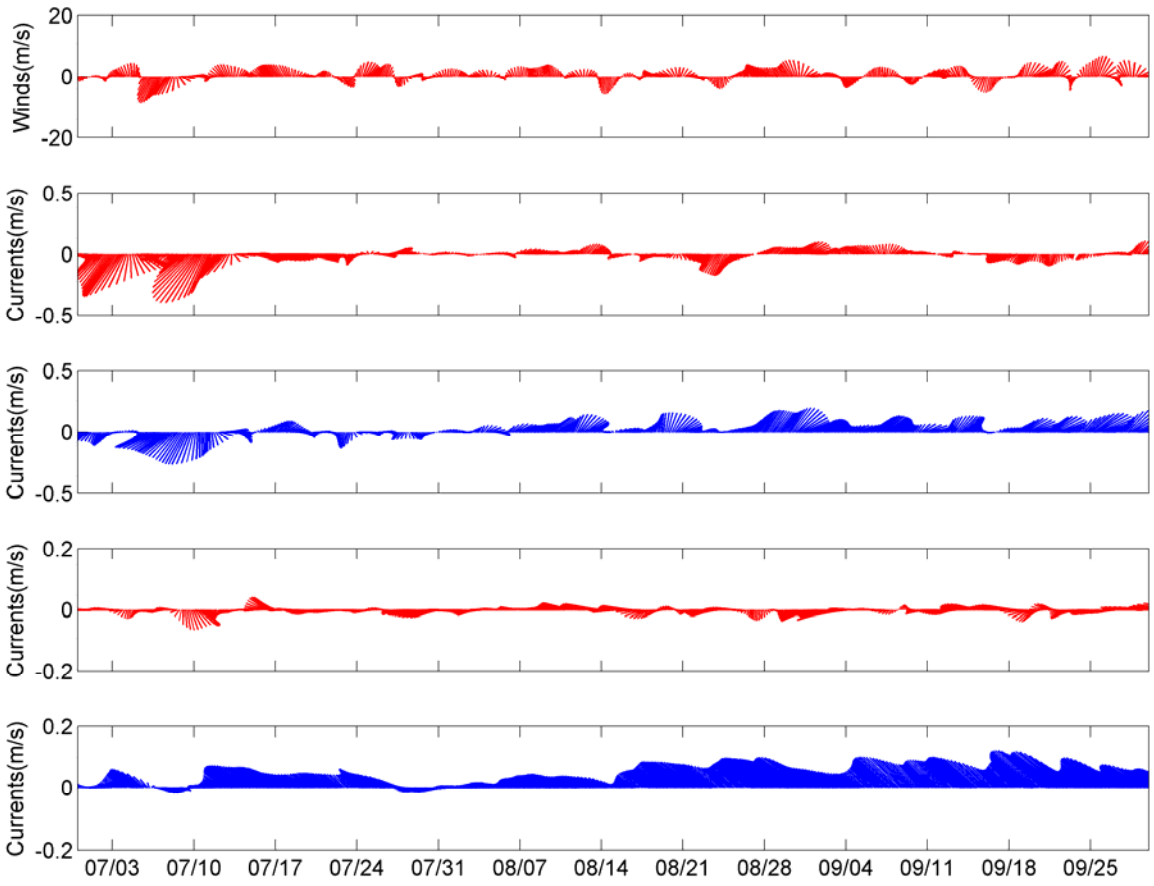

Figure 3.11. Winds at NOAA 44013 and currents at GoMOOS A in Jul.-Sep. From top to bottom panels: Winds, observed surface currents, modeled surface currents, observed currents at 50m, and modeled currents at 50m.

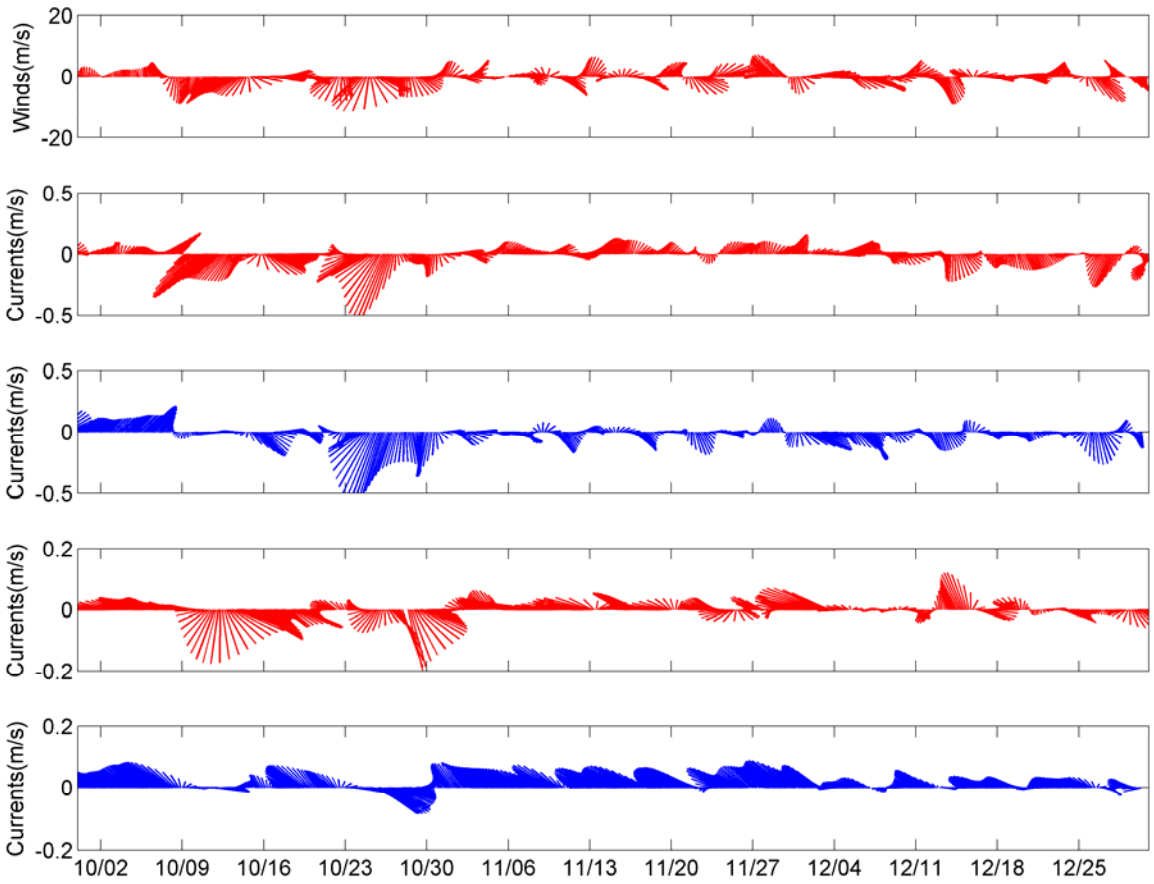

Figure 3.12. Winds at NOAA 44013 and currents at GoMOOS A in Oct.-Dec. From top to bottom panels: Winds, observed surface currents, modeled surface currents, observed currents at 50m, and modeled currents at 50m.

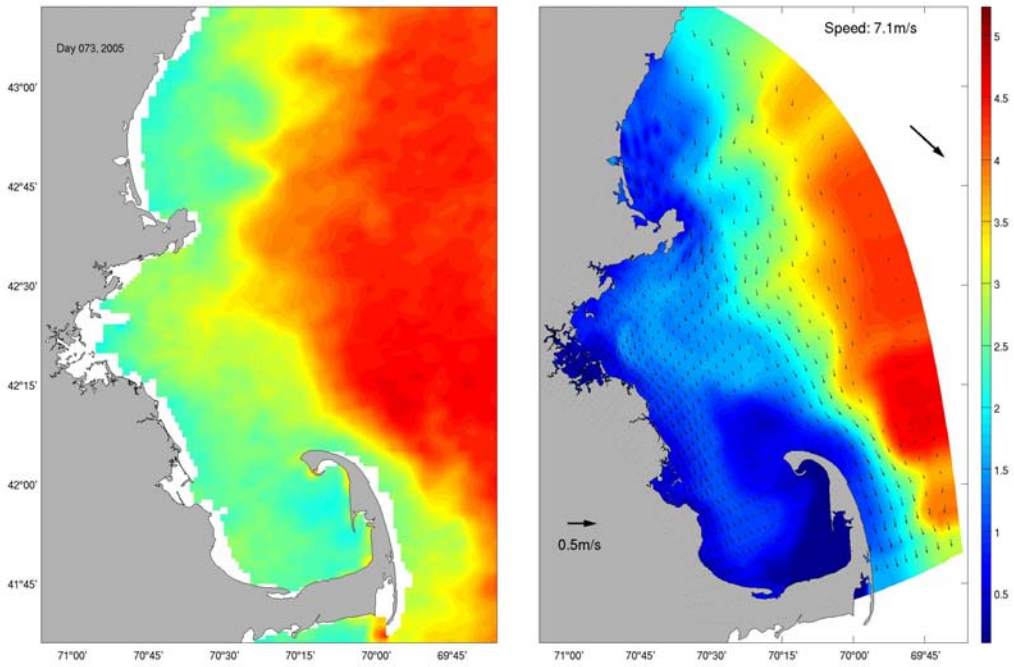

Figure 3.13. Sea surface temperature and currents on March 14, 2005. Left: SST from MODIS. Right: model SST (color) and surface currents (arrows). Daily mean wind vector (arrow in upper right corner) and wind speed are also shown.

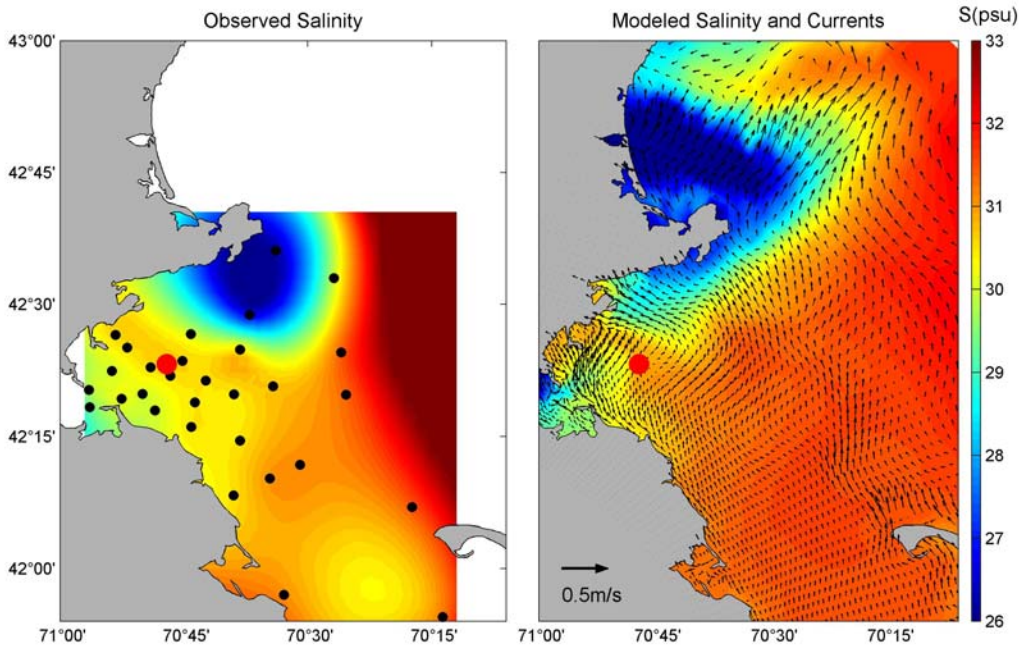

Figure 3.14 Surface salinity and currents in April 4-7, 2005. Left: survey data (black dots indicate survey stations). Right: model salinity (color) and currents (arrows). Model result is half-day average centered on April 6. The red dots indicate the outfall site.

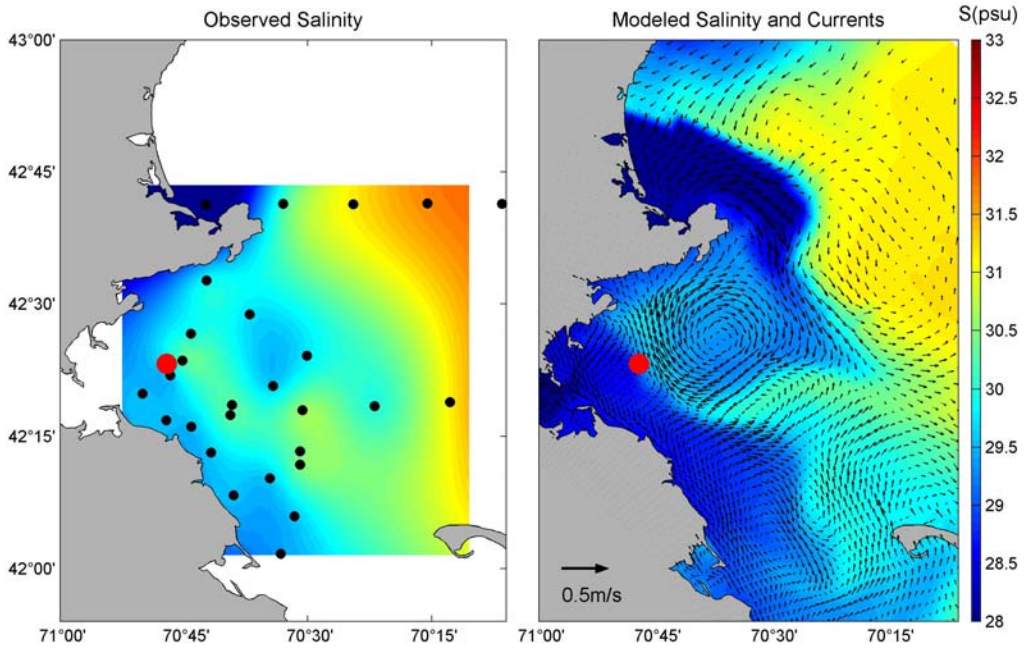

Figure 3.15 Surface salinity and currents in May 10-11, 2005. Left: survey data (black dots indicate survey stations). Right: model salinity (color) and currents (arrows). Model result is half-day average centered on May 11. The red dots indicate the outfall site.

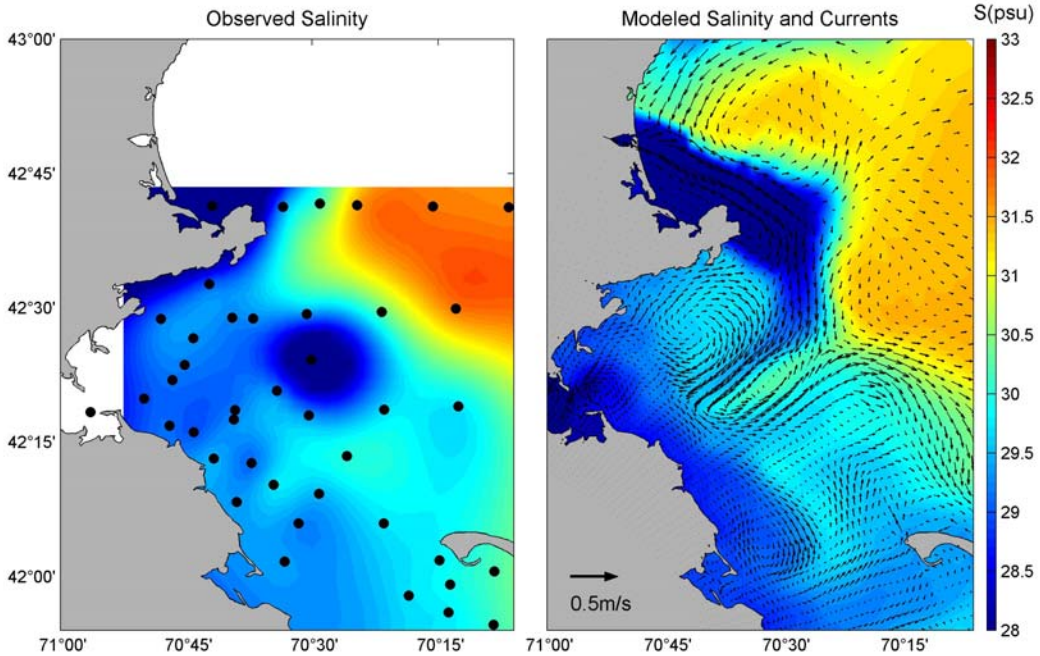

Figure 3.16 Surface salinity and currents in May 28-29, 2005. Left: survey data (black dots indicate survey stations). Right: model salinity (color) and currents (arrows). Model result is half-day average centered on May 28.

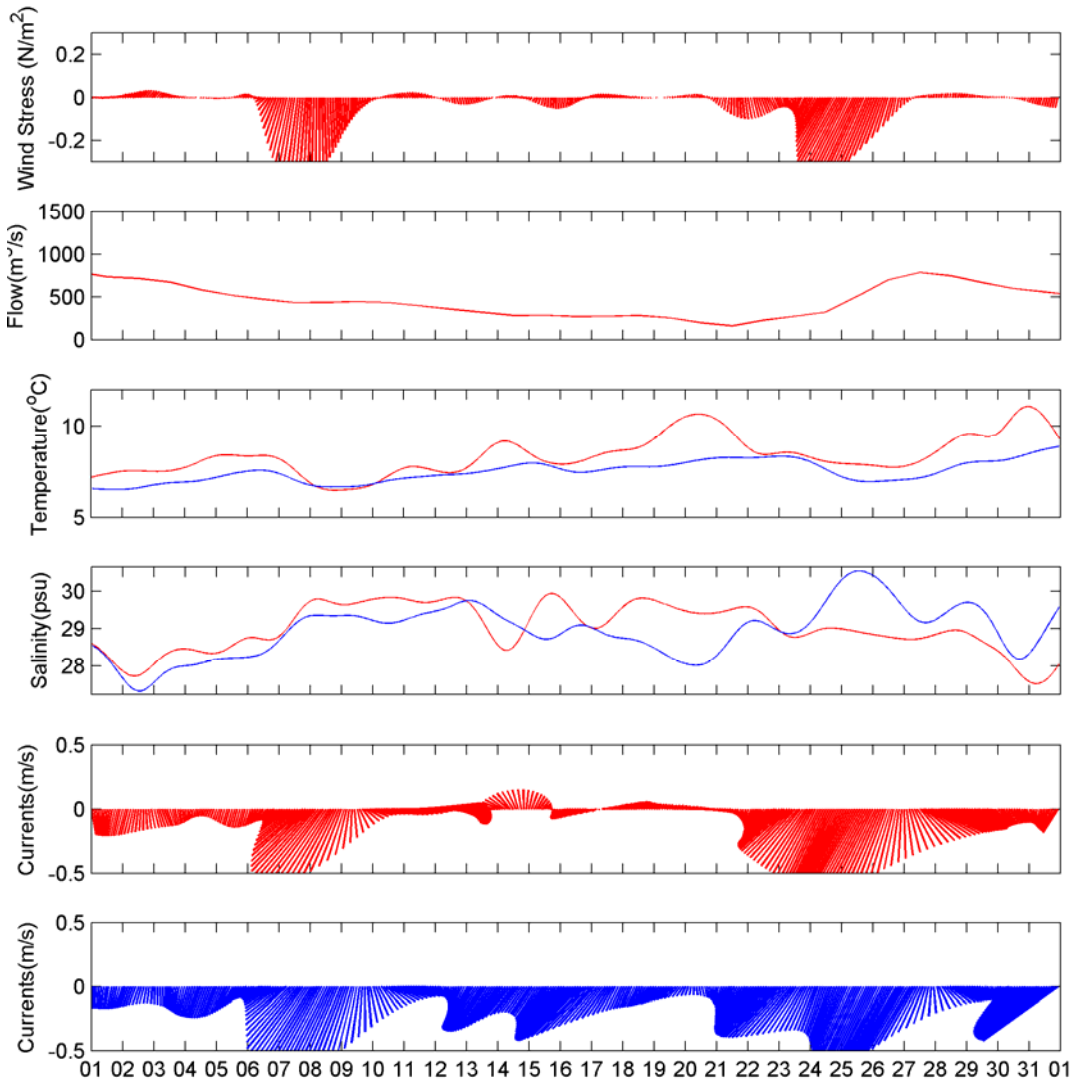

Figure 3.17 Wind stresses at NOAA buoy 44013, Merrimack River flow and surface physical conditions at GoMOOS buoy A in May 2005. From top to bottom: Wind stresses, river flow, temperature (red: data, blue: model), salinity (red: data, blue: model), observed currents, and modeled currents.

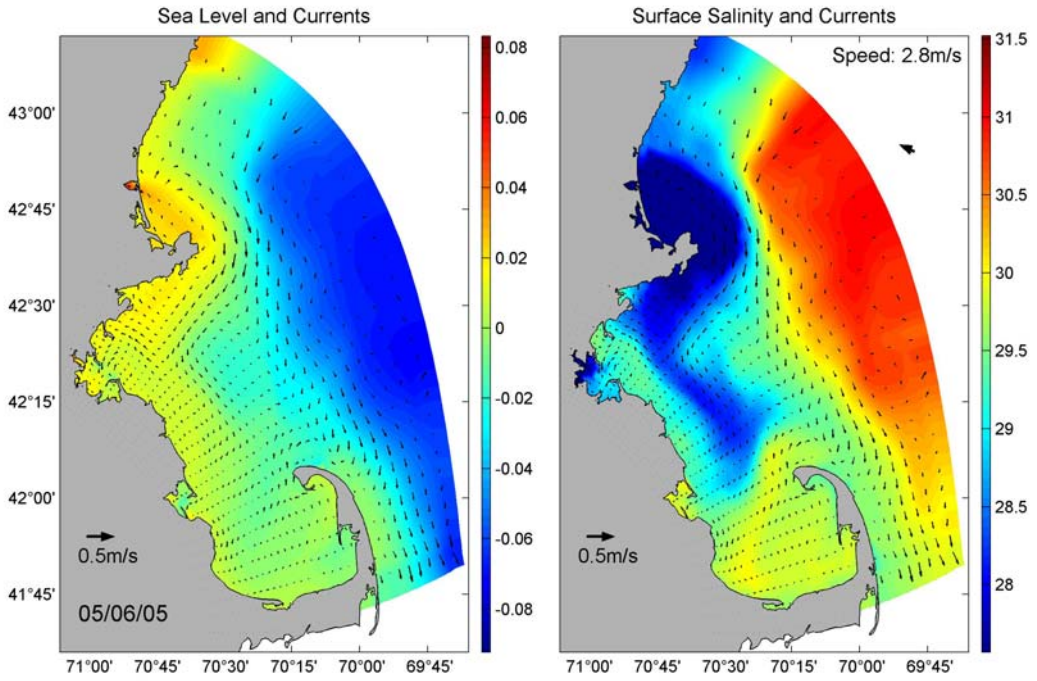

Figure 3.18 Sea surface elevation, salinity and currents on May 6, 2005. Left: sea surface elevation (color) and currents (arrows). Right: surface salinity (color) and currents (arrows). Wind vector (big arrow in upper right corner) and speed are also shown.

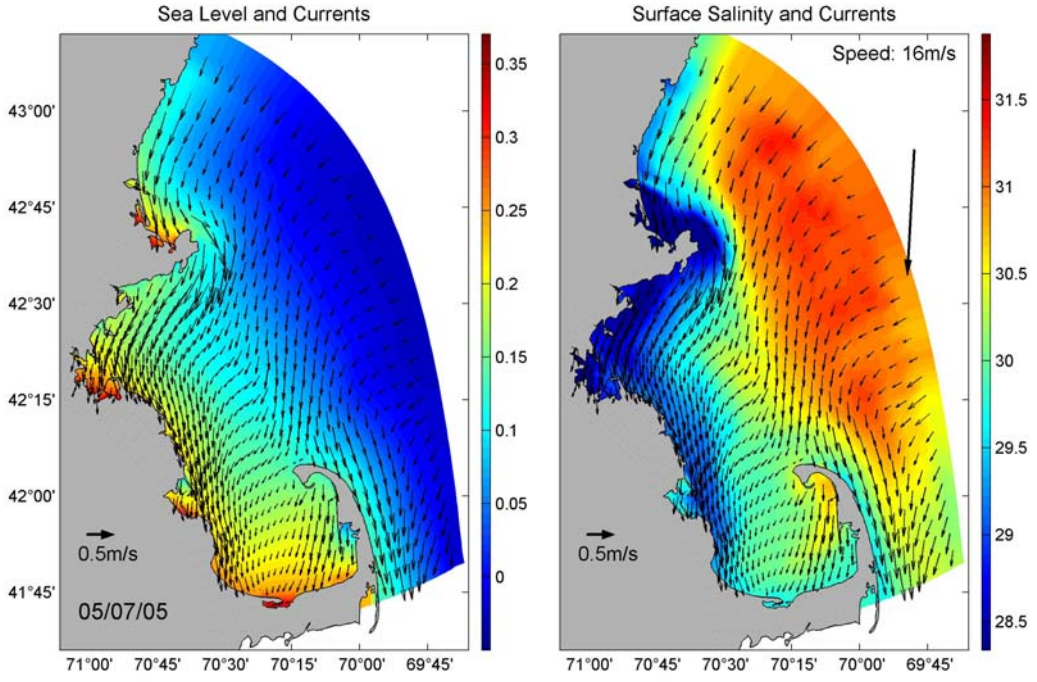

Figure 3.19 Sea surface elevation, salinity and currents on May 7, 2005. Left: sea surface elevation (color) and currents (arrows). Right: surface salinity (color) and currents (arrows). Wind vector (big arrow in upper right corner) and speed are also shown.

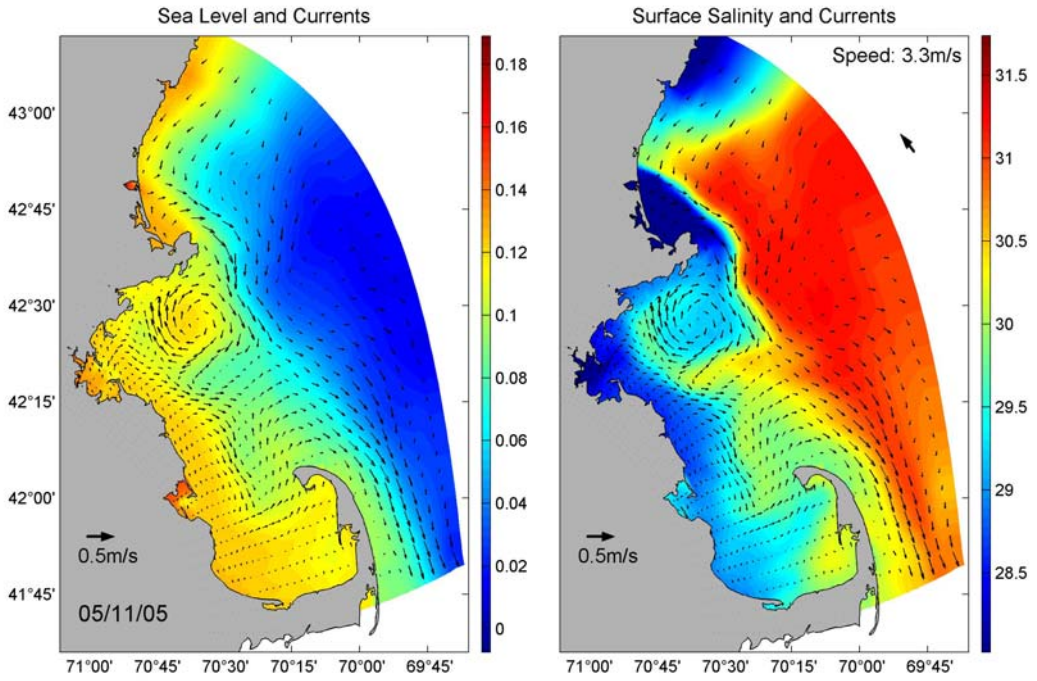

Figure 3.20 Sea surface elevation, salinity and currents on May 11, 2005. Left: sea surface elevation (color) and currents (arrows). Right: surface salinity (color) and currents (arrows). Wind vector (big arrow in upper right corner) and speed are also shown.

4. SUMMARY AND RECOMMENDATIONS

4.1 Summary

This report presents the validation of MBS hydrodynamic model results for 2005. Overall, modeled temperature, salinity and currents compared well with observations from moorings and surveys in terms of overall values, spatial patterns, and temporal evolution in response to both short-term and seasonal changes in meteorological forcing, freshwater inputs and boundary forcing. The validation and analysis of modeled results indicates again that the MB hydrodynamic model is robust and ready for applications in various environmental studies.

The model continues to experience difficulties in simulation of (1) summer processes including bottom currents and the response to upwelling/downwelling and (2) the magnitude, spatial pattern, and timing of responses to short-term events.

The discrepancies between model results and observations in temperature, salinity and currents in western MB suggest the need of more detailed open boundary conditions. The paucity of available data results in over-smoothed open boundary conditions which is likely the major cause of uncertainty in the modeled water exchanges between MB and the GOM. This can further lead to inaccurate simulation of the freshwater plume from the Merrimack River and other upstream rivers, and hence surface salinity in western MB. In 2005, more data were available during the spring when enhanced field surveys of MWRA and WHOI were conducted in response to the red-tide bloom. This allowed us to construct better boundary conditions and hence improve the simulation results.

This and previous analysis also suggest the need for studies on the freshwater plume dynamics near Cape Ann. Interactions between the topography, coastal currents, surface winds and freshwater plume are likely controlling the bifurcation and intrusion of WMCC near Cape Ann. Better simulation of this process will also improve the model capability in simulating the boundary exchange. Overall, a better understanding of this process and a model with higher resolution are needed to improve the simulation.

4.2 Recommendations

Improving open boundary conditions. The lack of short-term variability in the open boundary conditions will cause 1) weaker short-term variability in modeled currents, and 2) inaccuracy of salinity in western MB due to inaccurate simulation of freshwater plume from the

Merrimack River and other upstream rivers. Assimilation of measurements at GoMOOS buoy B has significantly improved the modeled salinity and currents. However, information along most of the open boundary is still lacking. Nesting the MB model in a GOM model may improve open boundary conditions and hence model results.

Improving both vertical and horizontal grid resolutions. The increase in horizontal resolution can lead to a decrease in grid-related horizontal numerical diffusion, an increase in horizontal density gradient, a better representation of baroclinic instability, and current-topographic interactions. For example, dynamic processes near Cape Ann may be improved with higher grid resolution that better resolves the bathymetry and frontal structure. Also, as noted before (Jiang and Zhou, 2006a), a higher resolution may improve the simulation of upwelling/downwelling front during upwelling/downwelling events, which is critical in simulating the strength, area extent, and timing of the responses.

Process studies. Analyses of model results and observations again suggests the needs for more process studies including (1) studies of meso-scale processes, (2) dynamic processes near Cape Ann, which is critical in the boundary exchange between the GOM and MB.

Application of the MB forecast. A near real-time forecast system has been developed by the UMB modeling team (http://www.harbor1.umb.edu/forecast). The system has been run successfully in the last two years and is being continuously improved. This system will be useful for the better design of field surveys during both scientific studies and emergency management responses to unexpected events because oceanic conditions are highly dynamic and constantly evolving.

5. REFERENCES

Bigelow, H.B. 1927. Physical oceanography of the Gulf of Maine (Part II). Bulletin of the Bureau of Fisheries, 40: 511-1027.

Blumberg, A.F. and G. L. Mellor, 1987. A description of a three-dimensional coastal ocean circulation model. In: Three-Dimensional Coastal Ocean Models, Coastal and Estuarine Sciences, Vol.4, N. Heaps (Ed.), American Geophysical Union, Washington, D.C., 1-6.

Butman, B., M.H. Bothner, F.L. Lightsom, B.T. Gutierrez, P.S. Alexander, M.A. Martini, and W.S. Strahle, 2002, Long-term Oceanographic Observations in Western Massachusetts Bay offshore of Boston, Massachusetts: Data Report for 1989-2000, U.S. Geological Survey Digital Data Series 74.

Casulli, V., 1990, Semi-implicit finite difference methods for the two-dimensional shallow water equations, J. Comput. Phys., 86: 56-74.

Galperin, B., L.H. Kantha, S. Hassid and A. Rosati, 1988. A quasi-equilibrium turbulent energy model for geophysical flows. J. Atmos. Sci., 45: 55-62.

Geyer, W. R., G.B. Gardner, W.S. Brown, J. Irish, B. Butman, T. Loder, and R.P. Signell, 1992. Physical oceanographic investigation of Massachusetts and Cape Cod Bays. Massachusetts Bay Program. MBP-92-03, 497pp.

Hagen, S.C. and D. M. Parrish, 2004, Unstructured mesh generation for the western North Atlantic tidal model domain, Engineering with Computers, 20(2), 136-146. DOI: 10.1007/s00366-004-0281-7

HydroQual, Inc. 2000. Bays Eutrophication Model (BEM): modeling analysis for the period 1992-1994. Boston, Massachusetts Water Resources Authority. ENQUAD 2000-02, 158pp.

HydroQual, Inc. and R.P. Signell, 2001. Calibration of the Massachusetts and Cape Cod Bays Hydrodynamic Model: 1998-1999. Boston, Massachusetts Water Resources Authority. ENQUAD 2001-12, 170pp.

Jiang, M. S. and M. Zhou, 2003. Massachusetts Bay Hydrodynamic Model and Water Quality Model results in 1998-99: Comparison Report between HydroQual and University of Massachusetts Boston Runs. Boston, Massachusetts Water Resources Authority. ENQUAD 2003-10, 42pp.

Jiang, M.S. and M. Zhou, 2004a, Calibration of the Massachusetts and Cape Cod Bays

Hydrodynamic Model: 2000-2001. Boston: Massachusetts Water Resources Authority. ENQUAD Report 2004-08. 71pp.

Jiang, M.S. and M. Zhou, 2004b. Calibration of the Massachusetts and Cape Cod Bays water quality model: 2000-2001. MWRA ENQUAD 2004-09. 90pp.

Jiang, M.S. and M. Zhou, 2006a, The Massachusetts and Cape Cod Bays hydrodynamic model: 2002-2004 simulation. Boston: Massachusetts Water Resources Authority. Report 2006-12. 128 p.

Jiang, M.S. and M. Zhou, 2006b, Bays Eutrophication Model: 2002-2004 simulation. Boston: Massachusetts Water Resources Authority. Report 2006-13. 126 p.

Large, W.G. and S. Pond, 1981. Open ocean momentum flux measurements in moderate to strong winds, J. Phys. Oceanogr. 11: 324-336.

Lynch, D.R., Naimie, C.E. and Werner, F.E., 1996. Comprehensive coastal circulation model with application to the Gulf of Maine. Cont. Shelf Res., 12: 37-64.

Mellor, G. and T. Yamada, 1982. Development of a turbulence closure model for geophysical fluid problems, Rev. Geophys. Space Phys., 20: 851-875.

Pedlosky, J. (1987), *Geophysical Fluid Dynamics*. Springer-Verlag, 710pp.

Shapiro, R., 1975. Linear filtering, Mathematics of Computation, 29, 1094-1097

Signell, R.P., H. L. Jenter, and A. F. Blumberg, 1996. Circulation and effluent dilution modeling in Massachusetts Bay: model implementation, verification and results. USGS Open File Report 96-015, U.S. Geological Survey, Woods Hole.

Smagorinsky, J. 1963. General circulation experiments with the primitive equations: I. The basic experiment. Monthly Weather Review, 91: 99-164.

Smolarkiewicz, P. K., 1984: A fully multidimensional positive definite advection transport algorithm with implicit diffusion. *J. Comput. Phys.*, 54: 325-362.

Taylor, D.I. 2005. Patterns of wastewater, river and non-point source loadings to Boston Harbor, 1995 - 2003. Boston: Massachusetts Water Resources Authority. Report 2005-08. 52 pp.

Weller, R., D. Rudnick and N.J. Brink, 1995. Meteorological variability and air-sea fluxes at a closely spaced array of surface moorings. J. Geophys. Res., 100: 4867-4883.

Xue, H. J., F. Chai, and N. R. Pettigrew, 2000. A model study of the seasonal circulation in the Gulf of Maine. J. Phys. Oceanogr., 30: 1111-1135.

Zhou, M. 2002. Test results of the Massachusetts Bay hydrodynamic model (Year 1994), University of Massachusetts Boston, Department of Environmental, Coastal and Ocean Sciences, ECOS 2002-2, 35 pp.

Massachusetts Water Resources Authority
Charlestown Navy Yard
100 First Avenue
Boston, MA 02129
(617) 242-6000
http://www.mwra.state.ma.us